INFORMATION TO USERS

This manuscript has been reproduced from the microfilm master. UMI films the text directly from the original or copy submitted. Thus, some thesis and dissertation copies are in typewriter face, while others may be from any type of computer printer.

The quality of this reproduction is dependent upon the quality of the copy submitted. Broken or indistinct print, colored or poor quality illustrations and photographs, print bleedthrough, substandard margins, and improper alignment can adversely affect reproduction.

In the unlikely event that the author did not send UMI a complete manuscript and there are missing pages, these will be noted. Also, if unauthorized copyright material had to be removed, a note will indicate the deletion.

Oversize materials (e.g., maps, drawings, charts) are reproduced by sectioning the original, beginning at the upper left-hand corner and continuing from left to right in equal sections with small overlaps.

Photographs included in the original manuscript have been reproduced xerographically in this copy. Higher quality 6" x 9" black and white photographic prints are available for any photographs or illustrations appearing in this copy for an additional charge. Contact UMI directly to order.

ProQuest Information and Learning
300 North Zeeb Road, Ann Arbor, MI 48106-1346 USA
800-521-0600

UMI®

Molecular Cloning and Characterization of Two *Arabidopsis thaliana* Sulfotransferases

Jason Boyd

A Thesis

In

The Department

Of

Biology

Presented in Partial Fulfillment of the Requirements

for the Degree of Master of Science at

Concordia University

Montréal, Québec, Canada

June 2001

ABSTRACT

Molecular Cloning and Characterization of two *Arabidopsis thaliana* Sulfotransferases

Jason Boyd

Concordia University, 2001

Two *Arabidopsis thaliana* sulfotransferases, *AtST4a* and *AtST6*, were identified through BLAST searches of The *Arabidopsis* Information Resource's (TAIR) database using *AtST1* as a query sequence. The intronless *AtST4a* was cloned via PCR from *Arabidopsis thaliana* ecotype Col-0 genomic DNA. A cDNA clone of *AtST6* was obtained and fully sequenced. *AtST4a* and *AtST6* were both cloned into the bacterial expression vector pQE30. The recombinant proteins expressed in *E. coli* were 42 and 40 KDa, respectively.

It was determined that AtST4a displayed specificity for various stereoisomers of brassinosteroids and their immediate precursors. Of all the brassinosteroids tested, AtST4a exhibits its highest affinity for (22*R*, 23*R*)-28-homobrassinolide, with an apparent K_m of 19.2 μM and a V_{max} of 34 pkatal mg^{-1}. The apparent K_m value for the sulfonate donor, PAPS, was found to be 0.4 μM. The enzymatic activity of AtST4a is neither affected by the presence or absence of the lactone moiety or the oxidation state of position 6 on ring B. Taken together our results indicate that the activity of AtST4a is dependent upon an α-configured A ring.

AtST6 was found to sulfonate a wide range of primary and secondary alcohols with unknown kinetics. Due to this broad affinity toward alcohols and the vast array of primary, secondary and tertiary alcohols naturally present in plants, it was not possible determine the natural substrate of AtST6 in this study.

Molecular characterization of *AtST4a* and *AtST6* revealed that the deduced protein sequence of both enzymes contain all the amino acids involved in PAPS binding and catalysis (Marsolais et al. 1995). Expression studies failed to determine conditions under which the genes preferentially expressed. However, the *AtST6* cDNA, GBGe166, was cloned from mRNA isolated from flower tissue. As expression analyses failed to detect *AtST6* transcript utilizing total RNA derived from mature flower tissue, it is likely that *AtST6* is both temporally and spatially regulated during flower tissue development.

Putative transgenic plants constitutively expressing *AtST4a* in the sense orientation produced a phenotype similar to that of the known brassinosteroid deficient mutants. A range of phenotypes were observed from, wild-type to dwarfism. This is most likely due to to variation in expression between transgenic plants resulting from differences in T-DNA copy number and integration site.

To Piya

ACKNOWLEDGMENTS

I would like to thank my supervisor, Dr. Luc Varin, for his friendship, guidance and the opportunity to work in his lab on this project. His years of patience and advice were a profound gift for which I will always be grateful. He provided a unique liberating environment and a financial commitment which I deeply appreciate.

Special thanks to Dr. Reg Storms and Dr. Bill Zerges for their helpful discussions and advice, in addition to their participation on my committee. I would also like to thank Dr. Paul Joyce for participating as my external examiner as well as for providing me with my big break in science.

I would like to thank the members of my lab; Dr. Frédéric Marsolais, Satinder Gidda, Dr. Diego Spertini, Dr. Frédéric Savard, Anastassia Tkatcheva, Travis Chalmers and Raffi Tonikian for the many thoughtful discussions on science, my project and for generally providing a comfortable academic environment.

I want to extend my thanks to Dr. Ragai Ibrahim for his support and encouragement and to the members of his laboratory; Dominique Anzellotti, Dr. Ingrid Muzac and Linda Huang who all contributed, in their own way, to making my stay at Concordia an enjoyable and memorable one.

I cannot thank my wife, Piya Sen, enough for the many years of support and companionship which greatly influenced and contributed to the completion of my academic history.

I would like to thank my parents for their support of my aspirations and years of encouragement. Mom, this writing is as much your achievement as it is mine. Dad, I am thankful for the guidepost you provided so that I may take the direction in life which most suits me. I am grateful to my uncle, Ed Hailio, who has always been there for me and continues to be an important mentor in my life.

Lastly, I wish to thank the Department of Biology for providing me the means to pursue my academic aspirations and for financial support through teaching assistantships.

TABLE OF CONTENTS

LIST OF TABLES

LIST OF FIGURES

LIST OF SCHEMES

LIST OF ABREVIATIONS

AmOAc	Ammonium acetate
AtST#	*Arabidopsis thaliana* sulfotransferase #
BAW	*n*-Butanol-acetic acid-water (6:2:2 v/v/v)
BL	Brassinolide
BLAST	Basic local alignment search tool
BnST#	*Brassica napus* sulfotransferase #
BR	Brassinosteroid
BRI1	Brassinosteroid insensitive 1, brassinosteroid cell surface receptor of *Arabidopsis thaliana*
cDNA	Complementary deoxyribonucleic acid
ChoST	Choline sulfotransferase
ClustalW1.8	Multiple sequence alignment program
CPD	Brassinosteroid 23α-hydroxylase of *Arabidopsis thaliana*
CS	Castasterone
Da	Dalton
ddH_2O	Double destiled, ultra-purified water
DEPC	Diethyl pyrocarbonate
DesulfoGI	Desulfoglucosinolate
DET2	De-etiolated2, steroid 5α-reductase of *Arabidopsis thaliana*
DHEA	Dehydroepiandrosterone
DMSO	Dimethyl sulfoxide
DNA	Deoxyribonucleic acid

dNTP	Deoxynucleotide triphosphates
DTT	DL-Dithiothreitol
DWF1	DWARF1, steroid oxido-reductase of *Arabidopsis thaliana*
DWF4	DWARF4, steroid cytochrome P450 mono-oxygenase/hydroxylase of *Arabidopsis thaliana*
DWF5	DWARF5, sterol Δ^7-reductase of *Arabidopsis thaliana*
DWF6	DWARF6, identical to DET2
DWF7	DWARF7, Δ^7-sterol C5 desaturase of *Arabidopsis thaliana*
EDTA	Ethylenediamine tetraacetic acid
EST	Estrogen sulfotransferase
EtOH	Ethanol
ExPASy	Expert protein analysis system
FST	Flavonol sulfotransferase
GA	Gibberellic acid
GC	Gas chromatography
Gi	Glucosinolate
HCl	Hydrochloric acid
Hg	Mercury
HPLC	High performance liquid chromatography
HSST	Hydroxysteroid sulfotransferase
IPA	Isopropanol
IPTG	Isopropyl β-D-thioglucoside
Kbp	Kilo base pair
LK	pea homologue of DET2

LKB	pea homologue of DWF1
MeOH	Methanol
MES	2-[N-morpholino]ethanesulfonic acid
$MgSO_4$	Magnesium sulfate
$MnCl_2$	Magnesium chloride
mRNA	Messenger ribonucleic acid
MS	Mass spectroscopy
MS	Murashige and Skoog salt mixture
NaCl	Sodium chloride
NaOAc	Sodium acetate
NaOH	Sodium hydroxide
Ni-NTA	Nickel-nitrilotriacetic acid
NMR	Nuclear magnetic resonance
$OD_{\#}$	Optical density at # nanometers wavelength
PAGE	Polyacrylamide gel electrophoresis
PAP	3'-phosphoadenosine 5'-phosphate
PAPS	3'-phosphoadenosine 5'-phosphosulfate
PCR	Polymerase chain reaction
pkatal	picomoles of product formed/second of reaction time
PLMF-1	Periodic-leaf-movement-factor-1
PST	Phenol sulfotransferase
RARO47	*Arabidopsis thaliana* sulfotransferase 1
RNA	Ribonucleic acid

RT	Reverse transcription
RNase A	Ribonuclease A
SDS	Sodium dodecyl sulfate
ST	Sulfotransferase
$T_{\#}$	Transgenic plant line at # generation
TAE	40mM Tris-acetate, 1mM EDTA electrophoresis buffer
TAIR	The Arabidopsis Information Resource (www.arabidopsis.org)
TBE	45mM Tris-borate, 1mM EDTA electrophoresis buffer
TBADP	Tetrabutylammonium dihydrogen phosphate
T-DNA	Transferred-deoxyribonucleic acid fragment
TE	Teasterone
TLC	Thin layer chromatography
Tris	Tris-[hydroxymethyl] aminomethane
TY	Typhasterol
UV	Ultraviolet

A. INTRODUCTION

Sulfotransferases (STs) are enzymes which catalyze the transfer of a sulfonate group to an acceptor substrate. Sulfotransferases are generally grouped according to their localization (Huxtable 1986). Membrane-bound sulfotransferases are generally localized within the Golgi apparatus and catalyze the sulfonation of glycosaminoglycans, glycolipids and tyrosines in proteins and peptides (Bowman et al. 1999; Kehoe et al. 2000). Although there are a number of membrane-bound STs which have been characterized from mammalian tissues, there is currently only one example attributed to plant species. This plant tyrosylprotein sulfotransferase (TPST) is involved in the biosynthesis of the peptide hormone phytosulfokine (Hanai et al. 2000), a plant growth factor which requires sulfonation for activity (Matsubayashi et al. 1999). The second group of sulfotransferases are soluble, cytosolic enzymes. These enzymes accept a variety of small organic molecules as substrates such as flavonoids, steroids and neurotransmitters, as well as various xenobiotics. Generally, cytosolic sulfotransferases can be arranged into two functional groups. The first group is involved in the detoxification of xenobiotics and/or endogenous compounds and generally display broad substrate specificities (Mulder et al. 1990). The second group participates in important metabolic functions such as steroid transport or inactivation and they exhibit strict specificity for their substrates (Strott 1996).

A substantial amount of data has been collected concerning both membrane-bound and soluble mammalian sulfotransferases. However, in plant systems, sulfotransferase enzyme research has lagged considerably. It is the goal of our lab to address this area of study by systematically identifying, cloning, expressing and

characterizing the biological function of all sulfotransferases from one plant species. To this end, we have chosen *Arabidopsis thaliana* as a model system. *Arabidopsis* is a small, robust plant, with a short life cycle, that is easily transformed and has been intensively studied using genetic techniques. However, the greatest advantage to working with *Arabidopsis* is the current international initiative to sequence its genome. With the advent of genomics and recent technological advancements in large scale sequencing, a novel and powerful tool was developed. Researchers can now identify all genes of a particular function within an organism in seconds using a BLAST search. As of December 14th, 2000, the *Arabidopsis* genome initiative was successfully completed.

In view of the recent development of the *Arabidopsis* genomic database (www.arabidopsis .org), the present study will deal with the following aspects:

1 The identification of two novel plant sulfotransferases of *Arabidopsis thaliana* using genomic-based tools.

2 The cloning and characterization of two novel plant sulfotransferases of *Arabidopsis thaliana* which catalyze the sulfoconjugation of brassinosteroid molecules and alcohols, respectively.

3 The production of *Arabidopsis thaliana* Col-O transgenic plants consitutively expressing the *Arabidopsis* sulfotransferase, *AtST4a*.

B LITERATURE REVIEW

The goal of this review is to illustrate sulfate activation, sulfonate transfer and the sulfotransferase (ST) enzymes which catalyze sulfoconjugation. The current state of knowledge concerning the number of STs in the *Arabidopsis thaliana* genome will also be reviewed, including their substrate specificities, homology to each other and their genomic distribution. As many of the results will focus on Brassinosteroids (BRs) as a substrate for the *Arabidopsis thaliana* sulfotransferase four (AtST4a), BR synthesis, modifications and regulation also will be described.

B.1 SULFONATION REACTION

The present review of the sulfonation reaction, the enzymes and their substrates will be limited to the cytosolic soluble enzymes of plants and animals with the exception of the gallic acid glucoside ST from *Mimosa pudica*.

B.1.1 Sulfate Activation

Before sulfoconjugation may take place, the obligate cosubstrate, 3'-phosphoadenosine 5'-phosphosulfate (PAPS), must be synthesized.

In the 1950's, it was established that the activated cosubstrate of the sulfonation reaction was PAPS. In 1958, Robbins and Lipmann described the synthesis of PAPS as a two-step process catalyzed by the enzymes, ATP sulfurylase and APS kinase. The reactions leading to sulfonate activation are as follows:

(1) $ATP + SO_4^{2-} \longrightarrow APS + PP_i$

(2) $APS + ATP \longrightarrow PAPS + ADP$

Scheme 1. PAPS biosynthesis.

In the first step of PAPS biosynthesis, inorganic sulfate and ATP are condensed to form adenosine 5'-phosphosulfate (APS). Pyrophosphate (PP_i) is released in the formation of APS and its subsequent hydrolysis by pyrophosphatases drives the reaction forward.

In the second step of PAPS biosynthesis, the phosphorylation of APS at the 3'-position is catalyzed by APS kinase, which uses ATP as a phosphate donor. Both ATP sulfurylase and APS kinase were isolated from spinach leaves and found to be present in a chloroplast-enriched fraction. After sonication, the enzymes were recovered from the supernatant, suggesting that PAPS synthesis takes place within the chloroplast stroma (Shaw et al. 1972; Burnell et al. 1973).

First discovered by Baumann in 1876, sulfoconjugates were considered excretory products as sulfoconjugated molecules are more water-soluble. Since this time, sulfoconjugation has been identified in many processes typically modulating the bioactivity of the target molecule. Sulfoconjugation requires an ST, an activated sulfonate donor (PAPS) and a recipient molecule. The most common target of sulfonation is the hydroxyl group. The general reaction is as follows:

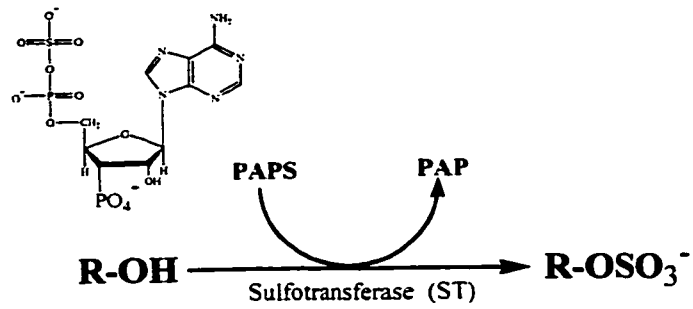

Scheme 2. General sulfoconjugation reaction.

B.1.2 Plant Sulfotransferases

In the past decade, a large number of plant STs have been characterized. Plant STs have a wide variety of substrate specificities and effects on their target molecules. Thus far, flavonols, desulfoglucosinolates, choline, gallic acid glucoside, BRs and hydroxy jasmonic acid have been identified as substrates for STs. A selection of STs from species other than *Arabidopsis* will be reviewed here.

Flavonoid Sulfonation

Flavonoids are important for UV-protection and in fighting against microbial attacks in plants. Flavonoids may also act as signal molecules which participate in the induction/inhibition of early nodulation genes in *Rhizobium* (Long 1989) and as regulators of polar auxin transport (Faulkner 1992). Binding of the napthylphthalamic acid (NPA) receptor by flavonol aglycones has been shown to inhibit the efflux of auxin from the basal end of the stem cells. However, flavonol conjugates, such as quercetin 3-sulfate, have been shown to block the quercetin-dependant accumulation of auxin.

To date, four position-specific flavonol STs from *Flaveria chloraefolia* and *Flaveria bidentis* have been isolated, cloned and biochemically characterized (Varin et al. 1989, Varin et al. 1991). These enzymes are specific for the hydroxyl groups at position 3 of flavonol aglycones, 3' and 4' of flavonol 3-sulfate, and position 7 of flavonol 3,3'- or 3,4'-disulfate. Furthermore, these sulfonation steps are carried out sequentially. The purified enzymes, similar to other plant STs, do not require divalent cations for activity, are not sensitive to SH group modifying reagents and have a molecular mass of 35 KDa. The K_m values of the four enzymes for substrates and PAPS varied between 0.2 and 0.4 μM.

Structure-function studies of the flavonol STs identified two strictly conserved residues important for catalysis and substrate binding. Residue, Lys^{59}, is involved in catalysis in the flavonol 3-ST as determined by site-directed mutagenesis and photoaffinity labeling experiments. It is presumed that Lys^{59} either acts to stabilize a reaction intermediate and/or to lower the activation energy of a transition state (Marsolais et al. 1995). Lys^{59} resides within conserved region I (Figure 1), located near the amino terminus of the protein, which has the consensus sequence TYP**K**^{59}SGTxW.

The second residue, Arg^{276} of the flavonol 3-ST, is absolutely required to form the PAPS-enzyme complex necessary for catalysis. Also confirmed by site-directed mutagenesis and photoaffinity labeling, this interaction is specific for the arginine side chain and Arg^{276} is thought to bind PAPS (Marsolais et al. 1995). Arg^{276} lies within conserved region IV, which has the consensus sequence **R**^{276}KGxxGDWKxxFT. Region

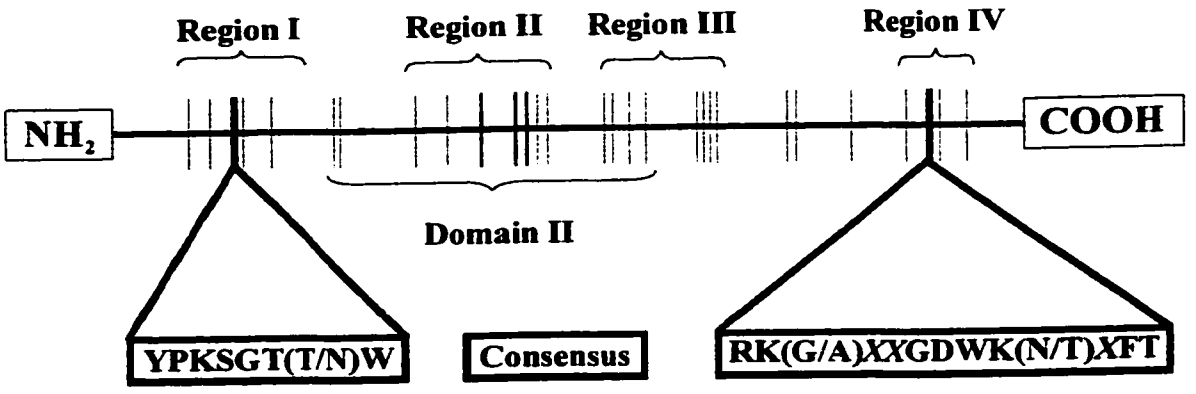

Figure 1. Schematic representation of the amino acid backbone of a generic ST depicting important conserved domains.

IV shows similarity with the p-loop motif (GxxxxGK) (Saraste et al. 1990), which is important for nucleotide binding in numerous enzymes. However, a few significant differences distinguish conserved region IV from the p-loop motif. There are additional conserved residues present at both extremities of region IV that are not present in the p-loop. Furthermore, spacing between the second glycine and lysine is absolutely conserved in the p-loop motif and is not maintained in region IV.

Studies with the flavonol 3- and 4'-STs have identified a domain involved in substrate recognition (Varin et al. 1995). This area, named Domain II, encompasses residues 92 to 194 and can be subdivided into a highly conserved region and two regions of high divergence.

Desulfoglucosinolate Sulfonation

GI STs (desulfoGI STs) are a class of secondary metabolites occurring in the Cruciferae family containing the important crop plant *Brassica napus* (canola) and the plant model system *Arabidopsis thaliana.* Feeding experiments have shown that glucosinolates (GIs) are derived from amino acids (Poulton et al. 1993). GIs are present in healthy plants, although their concentrations increase in response to mechanical wounding (Koristas et al. 1991) and fungal infection (Doughty et al. 1991). After tissue damage occurs, GIs are hydrolyzed by a thioglucosidase enzyme. This process results in glucose and a number of reactive products which are thought to enhance the plant's defence against micro-organisms and pests. These reactive metabolites also diminish the quality of products derived from *Brassica* such as canola oil and rape-seed meal used as

an animal feed, by degrading their nutritional content and taste quality. Therefore, GI reduction is of economic importance, especially to Canada.

To date, two desulfoGI STs have been purified from plant extracts. The first was purified from *Lepidium sativum* (cress) using gel filtration, affinity and ion-exchange chromatography techniques (Glendening et al. 1990). Purification resulted in an enzyme of ~31 KDa which proved to be unsTable and required the presence of bovine serum albumin to remain active. Like all plant STs, the purified enzyme required PAPS as the sulfonate donor for which it displayed a K_m of 60 μM. The enzyme catalyzed the sulfoconjugation of desulfobenzylGI (K_m 82 μM), desulfo-ρ-hydroxybenzylGI (K_m 670 μM), and desulfoallylGI (K_m 6.5 mM). All other potential substrates tested were not accepted by the enzyme. The low affinities for desulfo-ρ-hydroxybenzylGI and desulfoallylGI suggest that more than one enzyme may exist in plants, such as *Brassica napus*, accumulating significant concentrations of indolyl- and allyl- GIs.

A second desulfoGI ST was partially purified from *Brassica juncea* cell cultures by fractional precipitation with ammonium sulphate, anion-exchange chromatography and gel filtration (Jain et al. 1990). The purified enzyme displayed an apparent molecular mass of 44 KDa. The *Brassica* enzyme activity has no absolute requirement for divalent cations but does display strong inhibition by SH-group modifying reagents, as did the *Lepidium* enzyme, suggesting that one or more thiol groups are required for activity. The *Brassica* enzyme has a K_m of 2.3 and 0.78 μM for desulfobenzylGI and PAPS, respectively.

Choline Sulfonation

Plants of the Plumbaginaceae family live in areas of high salt concentrations and have adapted to this condition. All members of the family that have been studied accumulate choline sulfate (ChoS), which has been hypothesized to be an osmoprotectant. Early studies with *Limonium* species using *in vivo* radiotracer experiments demonstrated that [^{14}C]Choline (Cho) was converted to [^{14}C]ChoS, suggesting the presence of a ChoST (Hanson et al. 1991). Soon after this, the enzyme was purified from *Limonium sinuatum* root extracts. The ChoST is a soluble enzyme, more than 98% of its activity is recovered in the supernatant after centrifugation at 113 000 x*g* for 1 hr. The ChoST requires PAPS in order to sulfonate Cho and has K_m values of 5.5 and 25 μM for PAPS and Cho respectively (Rivoal et al. 1994). Choline sulfotransferase activity has been detected in all members of the genus *Limonium* that have been studied. No significant ChoST activity could be detected in plant species that do not accumulate ChoS such as barley, maize, sunflower, *Brassica* and *Arabidopsis*.

Gallic Acid Glucoside Sulfonation and Chemical Signals

Some plants have the ability to alter the orientation of their leaves in response to external stimuli. Examples of these movements include leaf closure at night (nyctinastism), solar tracking leaves (heliotropism) and leaf closure in response to mechanical stimuli (seismonasty). *Mimosa pudica* can perform both nyctinastic and seismonastic movements. Upon mechanical stimulus, electrical signals are involved in signal transmission from the site of perception to the motor organ (pulvinus) present at

the base of the petiole and leaflets (Satter 1990). Differential modification of cell turgor in the two halves of the pulvinus cause the leaves to decline, and their leaflets close 1 to 2 seconds after the plant is touched. The leaves recover their original position during a recuperation phase which takes between 2 to 5 min after the mechanical stimuli has ceased.

A substance that could induce leaf closing in *Mimosa* was identified as gallic acid 4-*O*-(β-D-glucopyranosyl-6'-sulfate) which was named Periodic-Leaf-Movement-Factor-1 (PLMF-1) (Schildknecht et al. 1981). Structure-activity studies revealed that PLMF-1 and other natural and synthetic derivatives required a sulfate group, a carboxyl group on the aromatic ring and a specific substitution pattern of the phenolic ring for biological activity (Kallas et al. 1989). A high-affinity binding site was later identified using sealed plasma membrane vesicles prepared from *Mimosa pudica* leaves (Kallas et al. 1990).

A model was proposed to explain the seismonastic response of PLMF-1 (Schildknecht et al. 1990). Based upon the similarity of action potentials between *Mimosa* and animal nerve cells, the induction of seismonasty with purified PLMF-1 and the identification of a stereospecific plasma membrane binding site, it was proposed that PLMF-1 functions in a similar manner to the neurotransmitter acetylcholine.

Later work identified a membrane-bound sulfotransferase from *Mimosa pudica* which catalyzes the transfer of a sulfonate group to gallic acid glucoside (Varin et al. 1997b). This enzyme catalyzes the final step in PLMF-1 biosynthesis and displays strict specificity and high affinity for both gallic acid glucoside (K_m = 3.0μM) and the sulfonate donor PAPS (K_m = 0.5μM). Enzyme activity was confined to the plasma membrane

preparations of the pulvini, indicating that the biosynthesis of PLMF-1 is limited to the motor organ (Varin et al. 1997b).

Brassinosteroid Sulfonation

Recently, an ST which catalyzes the sulfonation of brassinosteroids (BRs) was characterized from *Brassica napus* (Rouleau et al. 1999). *BnST3* was isolated from a *Brassica napus* genomic library using *Arabidopsis thaliana* sulfotransferase 1 (*AtST1* – also known as *RARO47*) (Lacomme and Roby 1996) as a probe. The BnST3 and AtST1 proteins share 87% amino acid identity (Rouleau et al. 1999). The enzyme BnST3, preferentially catalyzed the transfer of a sulfonate group to the OH group at position 22 of 24-epicathasterone, an intermediate in the biosynthesis of 24-epibrassinolide. The recombinant BnST3 did not catalyze the sulfonation of the structurally related mammalian steroids estrone, 17α-estradiol and testosterone. Similarily, BnST3 would not accept the phytosterols, campesterol, stigmasterol and β-sitosterol, nor the ecdysteroids ecdysone and 20-hydroxyecdysone (Rouleau et al. 1999). In-vitro enzymatic sulfonation of 24-epibrassinolide by recombinant BnST3 abolished its biological activity in the bean second internode bioassay (Rouleau et al. 1999). Normally, elongation of the second internode is observed when active BRs are applied to the base of the second internode. Expression studies using Northern and Western blot analysis determined that *BnST3* was induced with the application of salicylic acid, a signal molecule in the plants response to pathogen infection, suggesting that plants may respond to microbial attacks by modulating steroid-dependent, developmental processes. Experimental evidence

exists which suggests that BRs stimulate plant growth by increasing the plasticity of the cell wall (Clouse 1997), an undesirable phenomenon during pathogen infection as it facilitates the entry of the microbes.

B.1.3 Animal Sulfotransferases

There is now a large body of work concerning sulfotransferases of animal tissues. The majority of the research to date has focused on humans and rodents as model systems. This section will review a selection of enzymes characterized from these organisms. Sulfotransferases are members of a gene superfamily. In mammals, the enzymes catalyze the sulfonation of drugs, hormones and neurotransmitters. Cytosolic sulfotransferases are predominantly homodimers in mammals and monomers in plants, with molecular weights ranging from 30 to 36 KDa (Falany 1991; Weinshilboum et al. 1994; Varin et al. 1989; Kiehlbauch et al. 1995). The animal STs are classified into two families, the phenol STs and the hydroxysteroid STs, based upon amino acid sequence identities (Weinshilboum et al. 1994). Members of each family have a minimum amino acid sequence identity of 45%. Furthermore, the phenol ST family is subdivided into the phenol and estrogen STs, whose members share a minimum of 60% amino acid sequence identity. This classification system was modelled on the nomenclature system of the cytochrome P450s (Nebert et al. 1991).

Phenol Sulfotransferases

The phenol STs (PSTs) are important enzymes in mammalian tissues catalyzing xenobiotic and drug modification reactions. These enzymes play an important role due in part to their extensive tissue distribution, abundance and broad substrate specificities. PST activity in blood platelet cytosol is atributed to two phenol STs, P-PST and M-PST (Hart et al. 1979). At low substrate concentrations, P-PST specifically sulfonates natural phenols like *p*-nitrophenol (K_m= 0.5μM) and α-naphthol (K_m= 0.2μM), whereas M-PST sulfonates monoamine neurotransmitters such as dopamine (K_m= 1μM) and norepinephrine (K_m= 9μM). The human PSTs are thought to exist primarily as homodimers in their native form. However, it has been demonstrated that rat PSTs can exist as heterodimers (Kiehlbauch et al. 1995). It has been proposed that heterodimers of M-PST and P-PST in tissues may give rise to active enzymes with modified properties and may explain the phenomenon of multiple forms of PST activity observed during purification studies (Whittemore et al. 1985). M-PST has been purified from blood platelets and brain (Heroux et al. 1988, Whittemore et al. 1985) whereas P-PST has been purified from liver cytosol (Falany et al. 1990). The cDNAs of M-PST and P-PST have been cloned (Veronese et al. 1994) and encode proteins with molecular weights of 34.13 and 34.10 KDa, respectively. The two PSTs share 92.5% amino acid sequence identity.

Estrogen Sulfotransferases

Due to overlapping activities with the P-PSTs, it took some time to isolate and characterize the estrogen ST (EST) of humans. After the cloning of the cDNA (Aksoy et

al. 1993b), work on this enzyme progressed quickly. The EST migrates with a molecluar mass of 35 KDa during SDS-polyacrylamine gel electrophoresis (Falany et al. 1995). EST displays a high affinity for endogenous estrogens with maximal activities occuring with β-estradiol at low nanomolar concentrations (Falany et al. 1995). It is believed that estrogen sulfonation is involved in the inactivation of estrogen activity in target tissues (Hobkirk 1993). The EST also accepts structurally related estrogens as well as substrates for the DHEA-ST, such as DHEA and pregnenolone. However, these molecules are maximally sulfonated at micromolar concentrations (Falany et al. 1995). It has been demonstrated that EST can be induced by progesterone in the human endometrium during menstrual cycles (Clarke et al. 1982). This would have the effect of inactivating ovarian estrogens through sulfonation, which would otherwise have induced the release of an ovule. The crystal structure of the mouse estrogen sulfotransferase (mEST), in the presence of PAP, was the first ST structure to have been solved (Kakuta et al. 1997). As such, it has become an important tool for researchers studying substrate binding, catalysis and conformational properties. The mEST was originally cloned from mouse testes (Song et al. 1995a), where it probably protects this tissue from estrogen action.

Dehydroepiandrosterone Sulfotransferases

The dehydroepiandrosterone ST (DHEA-ST), also known as the hydroxysteroid ST, is the only hydroxysteroid ST present in human tissue (Falany 1997). DHEA-ST has been purified from human liver and adrenal tissues (Otterness et al. 1992; Falany et al. 1989) and its cDNA has been cloned from adult human liver mRNA (Otterness et al.

1992). Purified DHEA-ST migrates with a molecular mass of 35 KDa (Falany et al. 1989). To date, no post-translational modifications of DHEA-ST or any other human cytosolic ST have been reported. Size-exclusion chromatography of purified DHEA-ST illustrated that it exists as a homodimer (Otterness et al. 1992). The DHEA-ST enzyme preferentially accepts DHEA as a substrate (Falany et al. 1989) producing DHEA-sulfate. DHEA-sulfate is transported throught the blood serum and high levels of both DHEA and DHEA-sulfate have been associated with anti-obesity, anti-aging and anti-carcinogenicity in humans (Schwartz et al. 1988, Barret-Conner et al. 1986 and Majewska 1995). DHEA-ST is also capable of sulfonating the 3α- and 3β-hydroxyls of other hydroxysteroids, 3-phenolic hydroxyl group of estrogens, 17-hydroxyl group of testosterone and the 3 position of cholesterol (Aksoy et al. 1993a). DHEA-ST is thought to play an important role in the detoxication of bile acid secretions by the sulfonation of the 3α-hydroxyl position of amino acid-conjugated and free bile acids (Radominska et al. 1991). The DHEA-ST also catalyzes the sulfoconjugation of non-steroidal alcohols but with low affinity (Lyon et al. 1980).

Two distinct hydroxysteroid sulfotransferases (HSTs) have been isolated from the guinea pig adrenal (Driscoll et al. 1993). These two enzymes demonstrate substrate specificity with respect to the spatial orientation of the ring A 3-hydroxyl group. The 3βHST is a 33 kDa protein which will only accept substrates with a 3β-hydroxyl group. Similarily, 3αHST is a 32 kDa protein which will only accept substrates with a 3α-hydroxyl group. Neither enzyme sulfonates steroidal molecules having a planar ring A

configuration such as 17β-estradiol, nor do they sulfonate testosterone, cortisone and bile acids (Driscoll et al. 1993).

B.2 SULFOTRANSFERASES OF *ARABIDOPSIS THALIANA*

The goal of Dr. Luc Varin's research group is to characterize the biological function of each of the STs in the *Arabidopsis* genome. The work presented in this thesis involves the characterization of two *Arabidopsis* ST enzymes, *AtST4a* and *AtST6*. Therefore, it is necessary to include a discussion on the state of ST research in *Arabidopsis thaliana* and to illustrate the diversity of these enzymes. To that end, this section will provide a review of the current knowledge on the *Arabidopsis* STs, their identities with one another, as well as their genomic localization. The data concerning sequence identities and the genomic distributions of the *Arabidopsis* STs has been compiled from The Arabidopsis Information Resource's (TAIR) database (www.arabidopsis.org).

B.2.1 Functions/Activities

To date, seventeen *Arabidopsis thaliana* STs have been identified in the TAIR database with the Basic Local Alignment Search Tool (BLAST). The nomenclature adopted by the lab is to name each ST in consecutive order following the identification of their substrates. STs with unknown substrates may be subgrouped with other STs of known specificity, based upon a high amino acid sequence identity.

AtST1 (also known as *RARO47*, Genbank accession no. AC006836) was the first *Arabidopsis* ST cloned and characterized at the molecular level (Lacomme and Roby 1996). It was determined that *AtST1* is expressed in the aerial tissues of young seedlings. Treatment of *Arabidopsis* seedlings with salicylic acid and methyl jasmonate, stress-related compounds, revealed a rapid accumulation of *AtST1* mRNA transcripts. Furthermore, accumulation of *AtST1* mRNA was observed upon infection with bacterial pathogens (Lacomme and Roby 1996), in a similar manner to the induction of *BnST3* of *Brassica napus* (Rouleau et al. 1999). These data suggest that *AtST1* might play role in the plant-defence response to pathogen infection (Lacomme and Roby 1996).

AtST1 displays a high degree of sequence identity with the STs of *Flaveria* species (~42% identity) (Lacomme and Roby 1996). AtST1 and BnST3 share an amino acid sequence identity of 87%. All amino acids known to interact with the sulfonate acceptor, as described by the mouse estrogen sulfotransferase crystal structure (Kakuta et al. 1997), are identical between AtST1 and BnST3 except for the residues 180 and 181. Due to the significant amino acid sequence similarities between AtST1 and BnST3, it is likely that AtST1 is the *Arabidopsis* homologue of BnST3 (Rouleau et al. 1999). AtST1 shares ~40% amino acid identity with the remaining *Arabidopsis* STs and approximately 28% identity with the mammalian cytosolic soluble STs.

It was determined that AtST1, like BnST3, preferentially accepts 24-epicathasterone with a K_m and V_{max} of 6.9 μM and 57 pkatal mg^{-1} (Parez Y – unpublished). For a more detailed description of AtST1 enzymology, refer to section F.1.

The remaining *Arabidopsis* STs are presented in Table 1.

B.2.2 Identities, Dendrogram and Genomic Distribution of *Arabidopsis thaliana* Sulfotransferases

The matrix of amino acid sequence identities between all of the *Arabidopsis* STs and the dendrogram were generated with tools available at the Canadian Bioinformatics Resources web site (www.cbr.nrc.ca). Due to the limited sequence data available for *AtST11* (Genbank accession No. T51589), it was excluded from both the identity matrix and dendrogram presented in Table 2 and Figure 2. For a schematic of the chromosomal ST distributions, refer to Figure 3. In the following section the STs are presented as they appear on each chromosome.

Chromosome I:

Upon examination of the data compiled from the TAIR site on the *Arabidopsis* STs, a pattern emerges which is well represented by *AtST4b* and *AtST4c*. These two STs form the first of 5 ST gene clusters in the *Arabidopsis* genome who account for 11 of the 18 STs. These STs are positioned within 1kbp of each other and lie near the genetic marker, SBCSNP132. They share an amino acid identity of 77% and the dendrogram indicates that they are closely related. They also share a pattern with all the other clusters. All the ST clusters contain STs which are related to each other, and in general, share a high amino acid sequence identity.

Table 1. *Arabidopsis* ST summary.

Arabidopsis ST Designation	Substrate	Introns	Chromosome/ Genetic Marker	Cloned	References[a]
AtST1	24-epicathasterone	-	II mi320	Y	Lacomme et al 1996 Parez Y - unpublished
AtST2a	12-Hydroxy jasmonic acid	-	V mi97	Y	Gidda S – unpublished
AtST2b[b]	Hydroxyjasmonic acid	-	V mi97	Y	Tkatcheva A – unpublished
AtST3a	Flavonoid molecules	-	III TOPP5	Y	Gidda S – unpublished
AtST3b[b]	Flavonoid molecules	-	III TOPP5	N	Gidda S – unpublished
AtST3c[b]	Flavonoid molecules	3	II nga1126	N	Gidda S – unpublished
AtST4a	HomoCS	-	II mi398	Y	Boyd J – unpublished
AtST4b[b]	Brassinosteroids	-	I SGCSNP132	N	
AtST4c[b]	Brassinosteroids	-	I SGCSNP132	N	
AtST5a	Indol-glucosinolate	-	I PAB5 g14226	Y	Spertini D - unpublished
AtST5b	Aliphatic-Aromatic-Indol-glucosinolate	-	I PAB5 g14226	Y	Spertini D - unpublished
AtST5c[b]	Glucosinolate	-	I g15785	N	Spertini D - unpublished
AtST6	Alcohols	-	II mi320	Y	Boyd J – unpublished
AtST7	?	-	V mi83	N	
AtST8	?	-	II mi320	N	
AtST9	?	-	IV RP53	N	
AtST10	?	-	I m215 PAI3	N	
AtST11[c]	?	-	?	N	

[a] All unpublished results originate from the lab of Luc Varin.

[b] Substrate specificity is proposed due to sequence identity comparison to known STs.

[c] *AtST11* (Genbank accession No. T51589) is an ST that is induced upon infection with the cauliflower mosaic virus (CaMV) (Geri et al 1999). A partial cDNA was isolated whose translated sequence displayed a significant amino acid sequence identity with the flavonol STs of *Flaveria* species. The full-length gene has not been isolated, and its substrate specificity to date is unknown, however due to its pattern of induction, *AtST11* may be involved in the plant defense response to pathogen infection. *AtST11* has not been identified in the ABRC's database.

	AtST 1	AtST 2a	AtST 2b	AtST 3a	AtST 3b	AtST 3c	AtST 4a	AtST 4b	AtST 4c	AtST 5a	AtST 5b	AtST 5c	AtST 6	AtST 7	AtST 8	AtST 9	AtST 10	AtST 11
AtST 1	100																	
AtST 2a	44	100																
AtST 2b	42	85	100															
AtST 3a	47	40	42	100														
AtST 3b	45	38	39	85	100													
AtST 3c	44	39	39	80	83	100												
AtST 4a	42	39	37	59	58	58	100											
AtST 4b	44	42	41	64	63	64	72	100										
AtST 4c	42	38	38	61	61	63	85	77	100									
AtST 5a	37	36	35	40	37	37	36	38	37	100								
AtST 5b	38	34	38	41	39	37	38	38	36	74	100							
AtST 5c	40	34	35	41	38	37	35	38	35	72	76	100						
AtST 6	41	40	40	55	53	53	49	52	49	34	33	33	100					
AtST 7	44	41	40	65	63	63	60	61	61	38	39	37	54	100				
AtST 8	53	40	41	46	37	45	37	41	40	40	39	38	45	45	100			
AtST 9	44	38	38	62	58	62	52	54	54	37	37	37	53	61	44	100		
AtST 10	44	39	40	62	61	59	58	65	58	37	38	38	53	61	43	56	100	
AtST 11																		100

Table 2. Amino acid sequence identity matrix between all available *Arabidopsis* ST translated sequences.

Figure 2. Dendrogram of all STs from *Arabidopsis thaliana*. The tree was produced with the Phylip program available on the Canadian Bioinformatics Resource database.

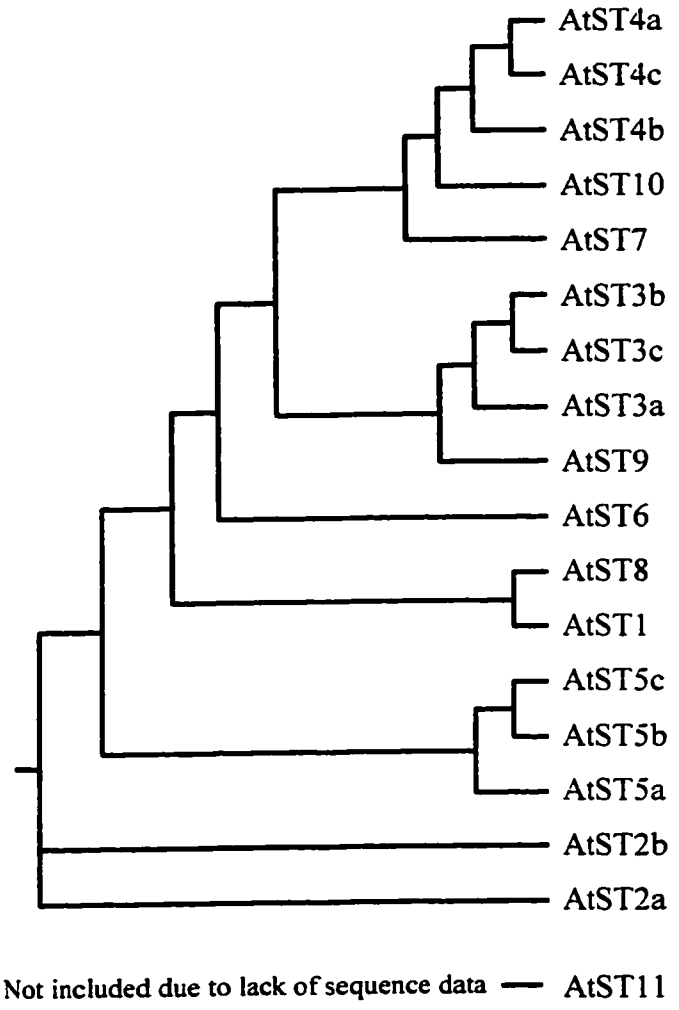

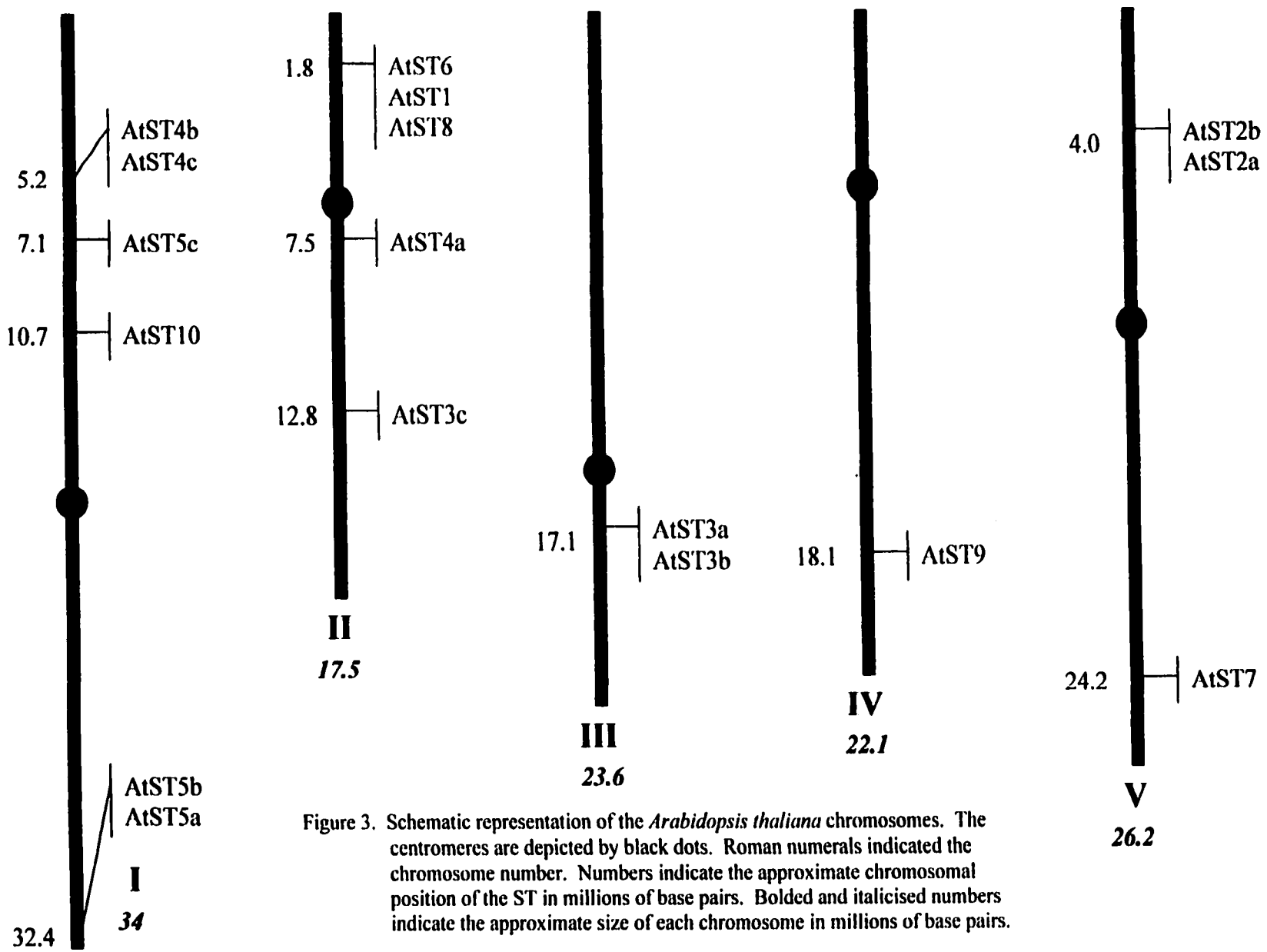

Figure 3. Schematic representation of the *Arabidopsis thaliana* chromosomes. The centromeres are depicted by black dots. Roman numerals indicated the chromosome number. Numbers indicate the approximate chromosomal position of the ST in millions of base pairs. Bolded and italicised numbers indicate the approximate size of each chromosome in millions of base pairs.

AtST5c and *AtST10* are both located on chromosme I, near the genetic markers g15785 and m215, repectively. They are not in close proximity to any other STs. *AtST10* shares its highest identity with *AtST4b* (65%) and is clustered with the *AtST4* genes and *AtST7* on the dendrogram. However, *AtST10* also shares 59% to 62% identities with the *AtST3* genes. It is clear from the dendrogram that the *AtST3* and *AtST9* gene cluster and the cluster comprising the *AtST4*, *10* and *7* genes are related and probably originate from a common ancestral gene.

AtST5a and *AtST5b* form another ST cluster whose amino acid sequence identities (74%) and substrate specificities are very similar. They lie within 300 nucleotides of one another and are in close proximity to the genetic marker g14226. This ST cluster displays another similarity shared with most of the other ST clusters. Three ST clusters, including this one, are composed of two similar genes and have a third related gene positioned elsewhere in the genome. In this case it is *AtST5c* which has identities of 72% and 76% with *AtST5a* and *AtST5b*.

Chromosome II:

AtST1 is localized on chromosome II, close to the genetic marker mi320, and is a member of the only ST cluster to contain three genes, including *AtST6* and *AtST8*. The composition of this cluster is similar to that of the others. Interestingly, *AtST8* shares its highest amino acid sequence identity with *AtST1* (53% identity) and is the only ST to show a significant relation to *AtST1* in the dendrogram. *AtST6* displays its highest

identity with the *AtST3*, *9*, and *10* genes. Similarly, *AtST6* may originate from an ancestral gene which is common to both *AtST9* and *AtST10*.

AtST4a and *AtST3c* are also located on chromosme II, near the genetic markers mi398 and nga1126, repectively. They are not in close proximity to any STs. Interestingly, the *AtST3* and *AtST4* genes share amino acid identities of approximately 61% with each other and form two destinct yet closely related clusters on the dendrogram.

Chromosome III:

AtST3a and *AtST3b* form another ST cluster which exhibit a high amino acid sequence identity (85%) and are believed to share similar substrate specificities. They are the only ST sequences present on chromosome III and are located near the genetic marker TOPP5. These genes are within 1.3 kbp of each other. This cluster also fits the pattern previously discussed, including that of a third related gene, *AtST3c*, present on another chromosome.

Chromosome IV:

AtST9 is the only ST sequence present on chromosome IV and is located near the genetic marker RP52. *AtST9* shares its higest identities with *AtST3a* and *AtST3c* (62%) and forms a cluster with the *AtST3* genes on the dendrogram.

Chromosme V:

AtST2a and *AtST2b* are members of another ST gene cluster localized to chromosome V, near the genetic marker mi97. The two open reading frames are separated by only 3 kbp. Both sequences are highly related (85% identity) and are therefore assumed to encode enzymes with similar substrate specificities. The *AtST2* genes share no more than 42% identity with the other STs.

AtST7 is present on chromosome V and is located near the genetic marker mi83. *AtST7* is an interesting gene as it shares 63% to 65% identities with the *AtST3* genes and 60% to 61% identities with the *AtST4* genes, in a manner similar to that of *AtST10*. Not surprisingly, *AtST7* and *AtST10* share a 61% amino acid sequence identity and are closely positioned on the dendrogram. *AtST7* clusters with the *AtST4* genes in the dendrogram and is also closely related to the *AtST3* genes.

B.3 BRASSINOSTEROIDS

The main focus of this thesis is to describe the work performed on the enzymes AtST4a and AtST6. AtST4a has been identified as a sulfotransferase accepting intermediates and end-products in the BR biosynthetic pathway. Therefore, it is necessary to provide a brief review of these molecules, their biosynthesis and known regulation. For a more comprehensive description of BRs, refer to the excellent review by Sakurai A., 1999.

In the early 1970's, researchers working for the United States Department of Agriculture (USDA) noted plant-growth promoting characteristics in *Zea mays* pollen

extracts. This activity was also identified in *Brassica napus* pollen (Mitchell et al. 1970). The authors noted a physiological response with extracts from 20 plant species when tested with the bean second-internode and the rice-lamina inclination bioassays. The response was unique from the other known plant hormones, auxin, cytokinins, gibberellins, abscisic acid and ethylene. The unknown plant-growth promoting element was named Brassin. In an effort to isolate the compound, researchers washed batches of *Brassica* pollen with water and then freeze-dried them prior to isopropanol extraction. The extract was partitioned with a two-phase solvent containing methanol, carbon tetrachloride and water. Methanol phases were pooled and purifed by silica gel chromatography. The fractions were further purified by silica gel and C_{18} column chromatography, and reverse-phase high-performance liquid chromatography. After crystalization, researchers (Grove et al. 1979) recovered 4 mg of Brassinolide (BL) from the equivalent of 40 kg of bee-collected pollen from *Brassica napus*. Crystal X-ray analysis of BL crystals revealed a steroidal structure, the first steroidal plant growth regulator.

Since this time, BRs have been detected at pmolar concentrations in hormone rich pollen, seeds and young vegetative tissues throughout the plant kingdom. BRs are difficult to detect in older tissues. BRs, like the structurally similar steroid hormones in mammals, elicit strong physiological responses from plants such as *Arabidopsis thaliana*, *Brassica napus* (canola), *Glycine max* (soybean), *Lycopersicon esculentum* (tomato) and *Pisum sativum* (pea). These include cell expansion and division, vascular tissue differentiation, inhibition of de-etiolation in the dark, repression of light-regulated genes

in the dark and repression of stress-regulated genes (Sala and Sala 1985, Mandava 1988, Clouse et al. 1993). Individuals deficient in or unable to perceive BRs display a pronounced dwarf phenotype - the *Arabidopsis thaliana* mutants, *de-etiolated2* (*det2*) and *brassinosteroid insensitive 1* (*bri1*), are good examples of the severity of these phenotypes (Li et al. 1996, Clouse et al. 1996).

The remainder of the review will focus on brassinosteroid biosynthesis and BR mutants followed by a discription of the known *in vivo* modifications of BRs.

B.3.1 Brassinosteroid Biosynthesis-Pathway

Brassinosteroids are terpenoid molecules, synthesized from mevalonic acid and squalene, a precusor in plant sterol biosynthesis. The BR biosynthetic pathway is more complex than that of the mammalian steroid hormones, which are derived from cholesterol and pregnenolone. BRs are derived from many plant sterol precursors (Benveniste 1986) and are classified as 27, 28 and 29 carbon steroids as seen in Figure 4. The variable number of carbons arise from variations in the side-chain structure, which is dependent upon the sterol precursor (Yokota 1997a). The 27 carbon norBRs are derived from cholesterol and lack a position 24 substituent. The 28 carbon BRs are synthesized from a number of sterols including 24-methylenecholesterol. The commonly occuring 28 carbon BRs, 24-epibrassinolide (24ß-methyl) and brassinolide (24α-methyl) are derived from 24-epicampesterol and campesterol, respectively. Finally, the 29 carbon BRs, which include 28-homobrassinolide (24 ethyl) and 28-homodolicholide (24-ethylidene), are synthesized from sitosterol and isofucosterol.

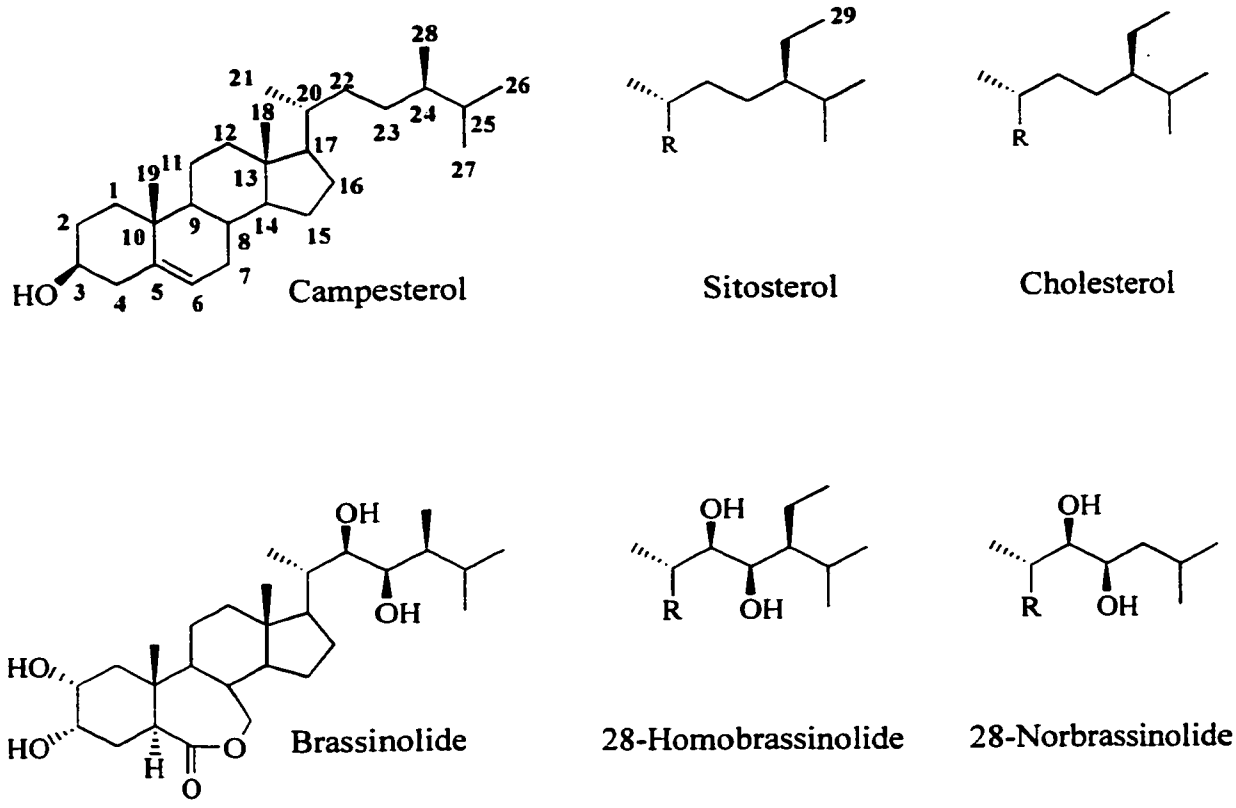

Figure 4. Plant sterol and brassinosteroid structures. Pictured are 27, 28 and 29 carbon molecules. Numbers system is illustrated.

Brassinosteroid biosynthesis has been elucidated with the aid of radio-labeled precursor feeding experiments and, more recently, confirmed with the aid of brassinosteroid biosynthetic mutants. A schematic of BL biosynthesis is presented in Scheme 3.

Initial studies utilizing cultured *Catharanthus roseus* cells (Suzuki et al. 1995a) and $^{13}C/^{14}C$-labeled campesterol, an abundant plant sterol (Figure 4), produced campestanol as the major metabolite. Conversion of campesterol to campestanol is a key step in BR biosynthesis (Fujioka et al. 1997).

Campesterol is converted to (24R)-24-methylcholest-4-en-3-one by dehydration of the 3β-hydroxyl followed by the isomerization of the $\Delta^{5(6)}$-bond. (24R)-24-methylcholest-4-en-3-one is then reduced to form (24R)-24-methylcholestan-3-one catalyzed by the de-etiolated2 (DET2) protein. Campestanol is produced from (24R)-24-methylcholestan-3-one by the reduction of the C3-ketone to a 3β-hydroxyl.

At this point, there is a branching in the biosynthetic pathway of brassinolide. From campestanol, the synthesis up to castasterone can proceed via the early or late C6-oxidation pathway.

In the early C6-oxidation pathway, campestanol is converted to 6α-hydroxycampestanol and then to 6-oxocampestanol as confirmed by chemically feeding deuterio-labeled campestanol and 6α-hydroxycampestanol to *C. roseus* cell cultures

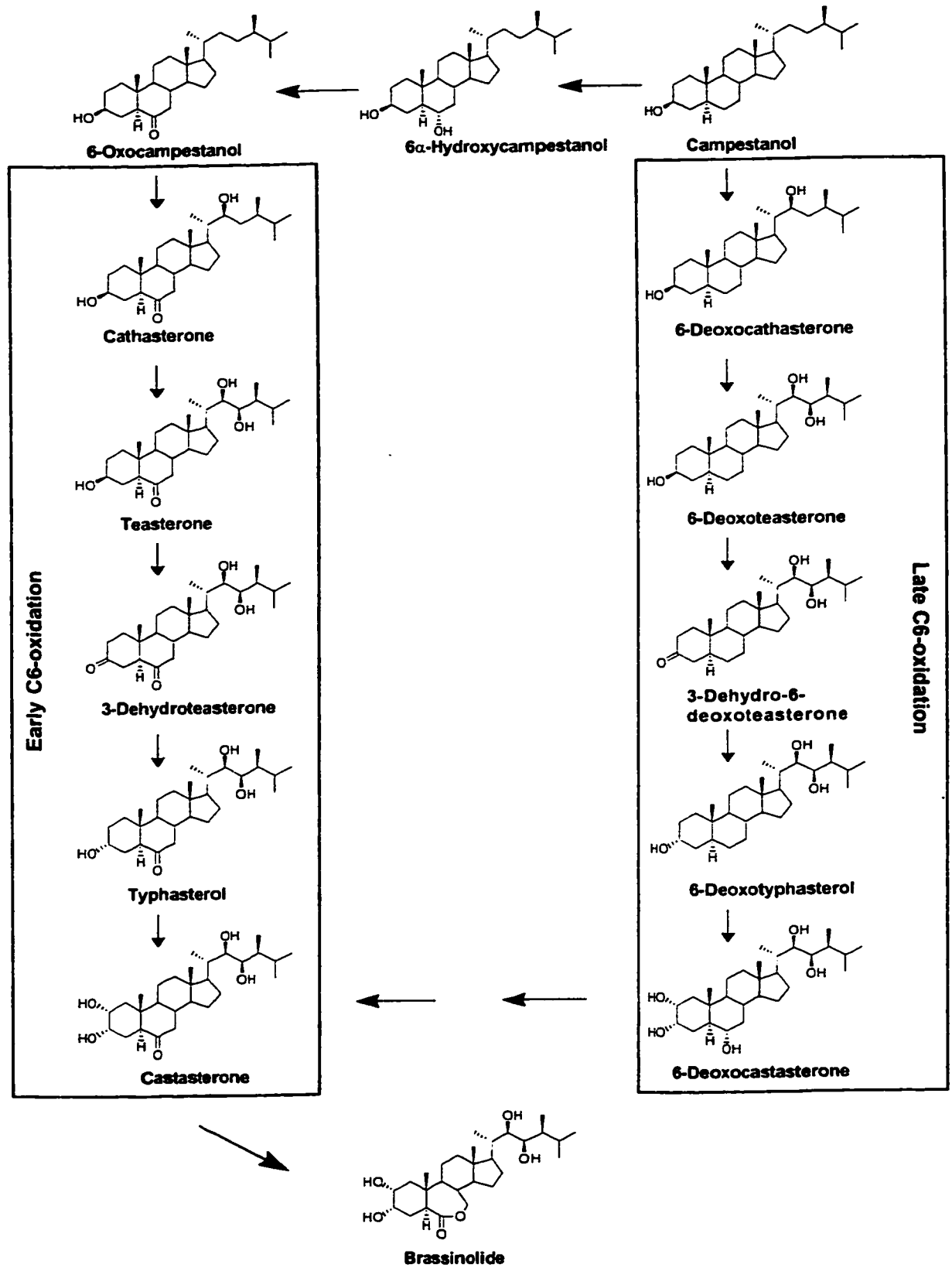

Scheme 3. Pathway of brassinosteroid biosynthesis.

(Suzuki et al. 1995a). 22α-hydroxy-6-oxocampestanol, commonly known as cathasterone, was identified with deuterio-labeled feeding experiments using *C. roseus* cell cultures, as an intermediate between 6-oxocampestanol and teasterone (TE) (Fujioka et al. 1995a). These feeding experiments with deuterio-labeled cathasterone also produced teasterone and typhasterol (TY). 6-oxocampestanol is hydroxylated at the C22 position to form cathasterone which is converted to teasterone by hydroxylation at C23. However, feeding experiments with deuterio-labeled 6-oxocampestanol have not detected cathasterone, as the cellular pool size of cathasterone was 1/500 that of 6-oxocampestanol. Therefore, this step in the biosynthetic pathway of brassinolide is assumed to be rate-limiting (Fujioka et al. 1995a).

Teasterone is converted to typhasterol in a reversible reaction with the inversion of the 3β-hydroxyl to a 3α-hydroxyl, also confirmed by feeding experiments in cultured cells of *C. roseus* (Suzuki et al. 1994a) and in the seedlings of *C. roseus*, *Oryza sativa*, and *Nicotiana tabacum* (Suzuki et al. 1995a). The intermediate BR, 3-oxo-3-dehydroteasterone, proved to be short-lived. Deuterio-labeled 3-oxo-3-dehydroteasterone produced typhasterol as the major metabolite with minor amounts of teasterone (Suzuki et al. 1994b). Endogenous 3-oxo-3-dehydroteasterone could not be detected in *C. roseus* but was identified as a natural BR in wheat grain (Yokota et al. 1994).

Feeding experiments with deuterio-labeled typhasterol showed that it is converted to castasterone by hydroxylation at position C2 in cultured cells of *C. roseus* (Suzuki et al. 1994a) and in the seedlings of *C. roseus*, *Oryza sativa*, and *Nicotiana tabacum* (Suzuki et al. 1995a).

In the late C6-oxidation pathway, 6-deoxocathasterone was thought to be a dead-end product as it did not display biological activity in BR bioassays. However, this changed when 6-deoxocastasterone was identified in cultured cells of *C. roseus* and was shown to be converted to castasterone and brassinolide in deuterio-labeled feeding experiments (Choi et al. 1996). Deuterio-labeled feeding experiments have also allowed the identification of the remaining 6-deoxoBRs intermediates.

Feeding experiments with deuterio-labeled precursors identified 6-deoxoteasterone and 6-deoxotyphasterol via the inversion of the 3β-hydroxyl to a 3α-hydroxyl. The deuterio-labeled intermediate, 3-dehydro-6-deoxoteasterone, produced 6-deoxotyphasterol in *C. roseus* cultured cells in a similar manner to that of the early C6-oxidation pathway. 6-Deoxotyphasterol is then hydroxylated at C6 to produce 6-deoxocastasterone, which is then oxidised to produce castasterone (Choi et al. 1996). 6-Deoxotyphasterol, 6-deoxocastasterone, typhasterol and castasterone, have also been identified in *Arabidopsis thaliana* (Fujioka et al. 1996). The intermediates in both pathways rescued the *Arabidopsis* BR deficient mutant *det2* (Fujioka et al. 1997), confirming that both the early and late C6-oxidation pathways play a role in plant growth.

Finally, the conversion of castasterone to brassinolide through the oxidation of the C_6-ketone was first demonstrated with feeding tritium-labelled castasterone to *C. roseus* cell cultures (Yokota et al. 1990).

B.3.2 Brassinosteroid Deficient Mutants

The identification and characterization of mutants defective in BR synthesis has proved to be a powerful tool for the dissection of the complex biosynthetic pathways. To date, all of the BR mutants isolated display a dwarf phenotype which can be distinguished from the dwarf phenotype of GA mutants. GA-deficient dwarf-mutants posses a shorter influorescence than BR-deficient mutants and many GA dwarfs fail to germinate in the absence of exogenously applied GAs. The known lesions in the BL biosynthesis pathway are presented in Scheme 4.

The first mutant, *dwf7*, displayed an endogenous sterol content similar to that of *dwf5*, it failed to accumulate campestanol, campesterol or 24-methylenecholesterol (Clouse and Feldmann 1999). Endogenous application of BR intermediates produced later in the pathway rescue the phenotype indicating that the steps from campesterol to BL are intact. It was determined that *DWF7* encodes a Δ^7-sterol C5 desaturase involved in the formation of the double bond between carbons 5 and 6, during the conversion of episterol to 5-dehydroepisterol (Choe et al. 1999) in the biosynthetic pathway leading to campesterol.

The *Arabidopsis* mutant *dwf5* is unusual in that all four of its alleles are fertile (Clouse and Feldmann 1999). The mutant phenotype results in the anthers being positioned closely to the stigmatic surface. The *DWF5* gene was mapped to the lower arm of chromosome I in *Arabidopsis*. Biochemical analysis of the endogenous sterol levels revealed that *dwf5* failed to accumulate campestanol, campesterol or 24-methylenecholesterol (Clouse and Feldmann 1999), suggesting a block before the

production of 24-methylenecholesterol (Scheme 4). Feeding experiments with a synthetic BR, 22α-hydroxycampesterol, and BR intermediates later in the pathway rescued the *dwf5* phenotype, indicating that the biosynthetic steps from campesterol to BL are not affected in this mutant (Clouse and Feldmann 1999). Recent work identified *DWF5* as a sterol Δ^7-reductase catalyzing the conversion of 5-dehydroepisterol to 24-methylenecholesterol (Choe et al. 2000). The DWF5 protein shares significant sequence homology with mammalian sterol Δ^7-reductases. However, the phenotype of *dwf5* mutant plants could not be rescued by the expression of the human sterol Δ^7-reductase.

The *Arabidopsis dwf1* mutant was the first T-DNA tagged mutant characterized in plants (Feldmann et al. 1989). Initial attempts to characterize *DWF1* failed to determine its function in plants. A second T-DNA tagged allele, *dim1* (*dwf1*), indicated that it contained a nuclear localization signal (Takahashi et al. 1995). It was later discovered that *DWF1* encodes an oxido-reductase (Genbank accession No. U12400) (Mushegian et at 1995). Feeding experiments with another allele of *dwf1*, *cbb1* (Kauschmann et al. 1996), showed that the mutant phenotype was rescued with the application of 28-homoBL, 24-epiCS and 24-epiBL. The conversion of 24-methylenecholesterol to campesterol is predicted to involve a two-step reaction, an isomerization of 24-methylenecholesterol to 24-methyldesmosterol and then a reduction to campesterol. Feeding experiments using deuterio-labeled 24-methylenecholesterol and 24-methyldesmosterol confirmed that *DWF1* acts at the reduction step between 24-methylenecholesterol and campesterol (Klahre et al. 1997). A BR mutant from pea, *lkb*,

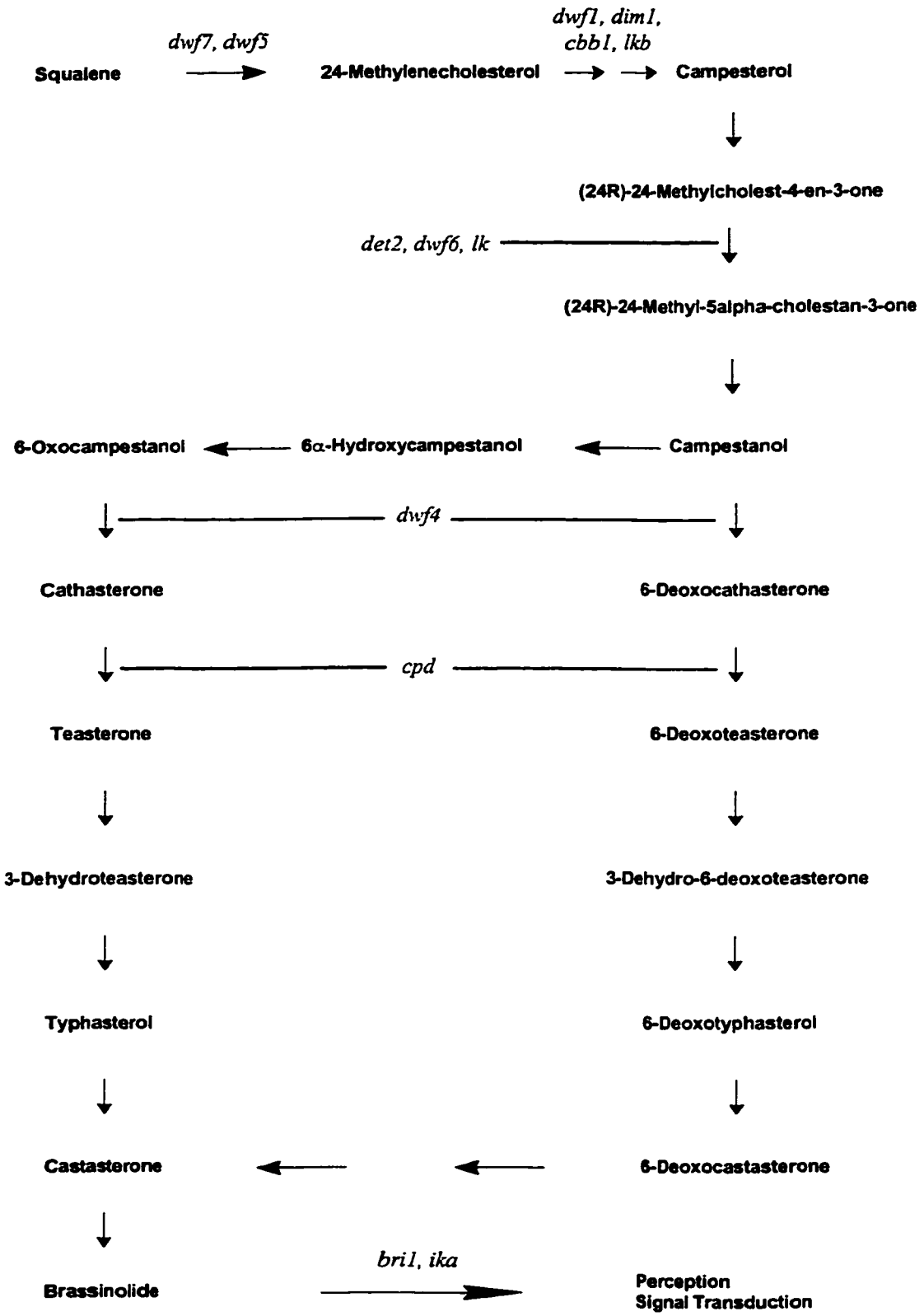

Scheme 4. Schematic of the locations of the BR mutants in biosynthesis and perception.

was isolated which had reduced levels of BL , CS, 6-deoxoCS, campestanol and campesterol but increased levels of 24-methylenecholesterol (Yokota et al.1997b). It has been suggested that *LKB* is the pea homologue of *DWF*1.

The conversion of campesterol to campestanol is an important reaction in the BL biosynthetic pathway and is the result of three reactions, dehydrogenation, isomerization and reduction (Li et al. 1997a). An *Arabidopsis* mutant has been isolated that is deficient in the reduction step (Li et al. 1996). This mutant, *det*2, maps to the bottom of chromosome 2 and was isolated in a screen for de-etiolated mutants, the phenotype for which it was named. The transformation of *det*2 mutants with human steroid 5α-reductases under the control of the CaMV 35S promoter (Li et al. 1996 and Li et al. 1997a) and the exogenous application of BRs, could rescue the phenotype. Similarly, the recombinant DET2 protein was able to reduce 3-oxo-$\Delta^{4(5)}$ mammalian type steroids, indicating that DET2 performs the same function in plants as do steroid 5α-reductases in humans. Quantification of the endogenous levels of BR intermediates in *det*2 mutants showed that there was an accumulation of (24*R*)-24-methylcholest-4-ene-3-one and reduction of approximately 90% of campestanol as compared to that of the wild type plant (Fujioka et al. 1997). Ten other alleles of *det*2 (*dwf*6) were isolated from T-DNA tagged mutant lines obtained from the Arabidopsis Biological Resource Center (ABRC) (Azpiroz et al. 1998). No mutants have been identified that affect the dehydrogenation or the isomerization steps of the campestanol conversion. However, low stringency screens for sequences similar to *DET*2 indicated that there is an homologous gene in the *Arabidopsis* genome. This was expected since some of the alleles of *det*2 accumulated

measurable levels of campestanol, suggesting the presence of a second reductase (Fujioka et al. 1997). A BR-deficient mutant of pea , *lk*, has been isolated, which exhibits reduced levels of campestanol and is suspected to be affected in a gene homlogous to the *DET2* gene of *Arabidopsis* (Yokota et al. 1997).

A BR deficient mutant has been isolated whose lesion occurs in the conversion of 6-oxocampestanol to cathasterone, a rate-limiting step in BL synthesis. This mutant, *dwf4*, has a de-etiolated phenotype when grown in the dark and the four known alleles are sterile or nearly sterile due to anthers that fail to reach the stigmatic surface (Azpiroz et al. 1998). *DWF4* maps to the lower arm of chromosome 4 (Azpiroz et al. 1998) and all four alleles appear to contain a loss-of-function mutation. Sequence analysis of *DWF4* suggests that it encodes a cytochrome P450 mono-oxygenase/hydroxylase (Choe et al. 1998). Feeding experiments using exogenously applied BR intermediates to *dwf4* seedlings determined that high concentrations of campestanol or 6-oxocampestanol failed to produce a response, however application of cathasterone and 6-deoxocathasterone could rescue the phenotype. Furthermore, *dwf4* seedlings were rescued to the wild-type phenotype with the application of 22α-hydroxycampesterol but not campesterol, suggesting that DWF4 can execute the hydroxylation of campestanol, 6-oxocampestanol and campesterol (Choe et al. 1998).

The *constitutive photomorphogenesis and dwarfism* (*cpd*) mutant of *Arabidopsis* was isolated from a screen of T-DNA tagged mutants and could be rescued with the application of teasterone (Szekeres et al. 1996). The mutant displays a light-grown phenotype and expressed a number of light regulated genes in the dark. In the light, *cpd*

plant height was just 3-5% that of the wildtype (Szekeres et al. 1996). *CPD* was mapped to the top of chromosome 5 in *Arabidopsis* and was found to encode a new class of enzymes in the cytochrome P450 gene superfamily (CYP90) of plants. *CPD* shares homology to specific domains of animal steroid hydroxylases (Szekeres et al. 1996) and exhibits an amino acid identity of 43% to *DWF4* (Choe et al. 1998). Neither *CPD* nor *DWF4* cluster with Group A plant cytochrome P450s (Choe et al. 1998) that catalyze plant-specific reactions, such as lignin biosynthesis. Non-A P450s share greater amino acid identity with P450s found in animals, microbes and fungi, and possess functions that are not limited to plants, such as steroid metabolism. Feeding experiments showed that *CPD* encodes a 23α-hydroxylase since the *cdp* mutant was rescued to the wildtype phenotype by BR intermediates hydroxylated at the C23 position and failed to be rescued by BR intermediates preceding teasterone (Szekeres et al. 1996). *CPD* gene expression is limited to cotyledons and leaf primordia of seedlings and in the adaxial parenchyma of expanded leaves in light-grown plants. Furthermore, BR intermediates carrying C22 and C23 side-chain hydroxyls regulate *CPD* gene expression through negative feedback inhibition. This inhibition is sensitive to cycloheximide treatment, a protein synthesis inhibitor, indicating a requirement for *de novo* synthesis of a regulatory factor (Mathur et al. 1998). Taken together, these results indicate that CPD catalyzes an essential reaction in BR biosynthesis. In addition, given that the expression of CPD is limited to specific tissues, it is likely that BRs are synthesized locally and then transported to their site of action.

Little was known about the mechanism of action of BRs as signals influencing plant growth and development. Screens for BR-insensitive mutants of *Arabidopsis* allowed for the isolation of more than 25 alleles of a particular locus (Clouse and Feldmann 1999). This gene, *brassinosteroid-insensitive* 1 (*BRI*1), was mapped to the bottom of chromosome IV near the polymorphic marker DHS1 (Clouse et al. 1996). Mutant *bri*1 plants exhibit multiple deficiencies in developmental pathways that include a severely dwarfed stature, thick dark green leaves, male sterility, reduced apical dominance and de-etiolation of dark grown seedlings (Clouse et al. 1996). Furthermore, the *bri*1 mutants could not be rescued with the exogenous application of BRs and did not respond to the presence of BRs in the hypocotyl elongation and primary root inhibition assays (Clouse et al. 1996). However, the *bri*1 mutants did retain their sensitivity to auxins, cytokinins, ethylene, abscisic acid and gibberellins (Clouse et al. 1996). *BRI*1 was found to encode a leucine-rich repeat receptor protein kinase (Li et al. 1997b) that was proposed to act as a brassinosteroid cell surface receptor. BRI1 has an extracellular domain with a leucine-rich repeat, a membrane-spanning domain, and an intracellular kinase domain whose target is unknown. Comparison to other plant homologues indicated that BRI1 contains a unique 70 amino acid island within the leucine-rich repeat that may function as a ligand binding domain. It is unknown whether BRs bind the receptor directly or whether BRs bind the receptor complexed to a steroid-binding protein. Futhermore, brassinosteroid binding to the extracellular domain of BRI1 has not been reported (Schumacher et al. 2000). The expression pattern of *BRI*1 indicates that the gene is expressed constitutively and in all tissues in light-grown plants (Li et al. 1997b).

The *bri*1 mutants, as well as the brassinosteroid-insensitive mutant of pea, *ika*, accumulate high levels of brassinosteroids as compared to wild-type plants (Noguchi et al. 1999, Nomura et al. 1999). As such, BRI1 must be required for the proper regulation of BR biosynthesis through feedback inhibition and may be involved in the negative feedback regulation of *CPD*.

*BRI*1 shares significant similarity with *Xa*21, a disease resistance gene isolated from rice (Song et al. 1995b). The extracellular leucine-rich repeat domain of *BRI*1 also shares a high degree of similarity with many plant resistance genes (Baker et al. 1997), suggesting that there may be an interaction between the steroid-signaling pathway and the disease resistance pathways. In order to test the function/activity of the BRI1 receptor domain, the extracellular and transmembrane domains of BRI1 were fused to the cytoplasmic serine/threonine kinase domain of Xa21 (He et al. 2000). Rice cells expressing the chimeric receptor activated the plant defence response against pathogen infection when treated with exogenous BRs. The experiment confirmed that the extracellular and transmembrane domains of BRI1 are functional and may be activated by BRs in an unknown fashion. At present however, there is no biochemical evidence that the cytoplasmic domain of the *BRI*1 gene encodes a functional kinase (Li et al. 1997b). It is evident that in order to better understand BR signal transduction, it will be necessary to determine whether the BRI1 receptor exists in a homo- or heterodimeric state and to identify the protein substrates that interact with the BRI1 kinase domain.

B.3.3 Brassinosteroid Metabolism

The metabolism of BRs is a topic that has received much attention in the last decade. However, detecting and studying BRs *in vivo* presents a number of difficulties. The most noTable problem is that BRs are present at very low concentrations in vegetative tissue with concentrations ranging from a few micrograms to submicrogram levels per kilogram of fresh weight. Therefore, most studies rely upon radioactive or heavy isotope-labeled precursors as well as mass spectroscopy (MS) and gas chromatography-mass spectroscopy (GC-MS) to detect metabolites.

A second problem arises with the choice of plant material. Intact plants and explants accumulate relatively low levels of metabolites due to uptake and transport barriers, yet more accurately reflect metabolic reactions that would naturally occur in a plant system. Cells cultures, on the other hand, tend to produce greater levels of metabolites and are cultivated in an aseptic environment, free of microbial influence, however, they do not accurately reflect the dynamics of a plant system.

In mung bean explants, feeding experiments with [^{3}H]-CS produced, as a major component, water-soluble metabolites determined to be non-glycosidic given that free BRs failed to be released upon treatment with pectolyase. The remaining hydrophobic metabolites displayed characteristics of glycoside-like metabolites which recovered their biological activity after hydrolysis by pectolyase. In comparison, [^{3}H]-BL was largely converted to [^{3}H]-23-*O*-β-D-glucopyranosyl-BL and nonglycosidic metabolites occurred only in minor amounts (Suzuki et al. 1993a).

Feeding experiments with rice seedlings have demonstrated that the major components of [^{3}H]-CS and [^{3}H]-BL metabolism were water-soluble, non-glycosidic compounds. Due to their sensitivity to solvolysis and to their chomatographic behaviour, it was suggested that these water-soluble compounds were BR sulfate esters. Similar results were obtained by alkaline hydrolysis of the [^{3}H]-CS metabolites (Yokota et al. 1992).

Application of a mixture of [^{3}H]-CS and [$^2H_6$]-CS to seedlings of *O. sativa* and *N. tabacum*, resulted in the epimerization of the 3α-hydroxyl to a 3β-hydroxyl, producing 3-epiCS (Suzuki et al. 1995b). This epimerization has previously been described in *P. vulgaris* seeds (Kim 1991) and results in a loss of biological activity. Metabolites undergoing such a modification are assumed to be inactivation products rather than biosynthetic products.

Feeding experiments using cucumber seedlings showed that the exogenously applied [^{14}C]-24-epiBL was metabolized differently in the leaves and epicotyls. A mixture of metabolites with varying polarities as compared to [^{14}C]-24-epiBL, was found in the leaves. However, in the epicotyls, only less polar metabolites were detected. Hydrolysis and MS data indicated that the polar metabolites were likely glucosides and that the less polar metabolites were acyl conjugates of [^{14}C]-24-epiBL, epimeric at a single position on the A ring (Nishikawa et al. 1995). The authors discuss the possibility that the conjugate may be either 2,24-epiBL or 3,24-epiBL. A later study indicated that only BRs having a 3β-hydroxyl group, and not a 3α, such as 3,24-epiBL, can be conjugated at the 3-position (Kolbe et al. 1998).

Application of [^{3}H]-22,23,24-triepiBL to hydroponically grown tomato plants indicated that as many as three metabolites were formed which were more polar than that of the parent compound (Schlagnhaufer et al. 1991). The structure of these metabolites was not investigated.

Studies using cell cultures of *O. sativus* have uncovered interesting BR metabolites. The BRs, [^{3}H]-24-epiCS and [^{3}H]-24-epiBL, were applied to cell cultures of *O. sativus* and incubated for 7 days before extraction of the culture medium with chloroform (Kolbe et al. 1994). A major peak was identified by thin layer chromatography (TLC) and purified by reverse phase HPLC. The structures defined with EI-MS and NMR spectroscopy indicated the presence of non-derivatized metabolites and acetyl derivatives. The loss of the side chain was observed for metabolites of both [^{3}H]-24-epiCS and [^{3}H]-24-epiBL. After the application of both [^{3}H]-24-epiCS and [^{3}H]-24-epiBL, intermediate metabolites containing a 20*R*-hydroxyl group were isolated at very low levels, suggesting a transient accumulation. The bond between C-20 and C-22 would be destabilized by the 20*R*-hydroxyl group, becoming accessible to enzymatic attack and ultimately cleavage. This method of steroid side chain degradation proceding via 20-hydroxylation has been previously described for 20-hydroxyecdysone in insects (Galbraith et al. 1969) and in crustaceans (Lachaise et al. 1984).

To better understand the mechanism of side chain degradation in *O. sativum*, [^{3}H]-24-epiBL was applied to cell cultures and metabolites were extracted after only a 24 h incubation period (Kolbe et al. 1995). MS and NMR spectroscopy data indicated that the

major metabolite in the culture medium was 3,24-diepiBL, suggesting that the epimerization of C-3 is the first step for BR metabolism in *O. sativum* (Scheme 5). Similar results were obtained when [^{3}H]-24-epiCS was applied (Kolbe et al. 1996). The major metabolite was identified as 3,24-diepiCS.

The metabolism of BRs in tomato (*Lycopersicon esculentum* L.) cell cultures has also received much attention. Feeding experiments using [^{3}H]-24-epiTE, which has a 3β-hydroxyl, showed that it is quickly converted to a hydrophilic glucoside. Five hours after application, 67% of [^{3}H]-24-epiTE was conjugated to a glucoside and only 33% of 24-epiTE was still present (Kolbe et al. 1997). This conjugation occurs exclusively at the 3β-position as detected by NMR. NMR analysis also identified the sugar moieties as β-D-glucopyranosyl-(1→6)-β-D-glucopyranoside (gentiobiose), β-D-glucopyranosyl-(1→4)-β-D-glucopyranoside (lycobiose) (Kolbe et al. 1997) and β-D-glucose (Kolbe et al. 1998b).

Radio-labeled [^{3}H]-24-epiCS was fed to tomato cell cultures in order to demonstrate Bayer-Villiger oxidation to produce the lactone ring and thus 24-epiBL (Hai et al. 1996). HPLC fractionation allowed the isolation of two glucosidic metabolites that were analyzed by NMR and MS. The metabolites were identified as 25-β-D-glucopyranosyloxy-24-epiCS and 26-β-D-glucopyranosyloxy-24-epiCS. It was determined that the hydroxylation reaction at positions C-25 and C-26, was a rate-limiting step, given that neither 25-hydroxy- nor 26-hydroxy-24-epiCS could be detected. Then, glycosylation followed as the fast-step.

Scheme 5. Metabolism of 24-epiBL in cell suspension cultures of *Ornithopus sativus* (serradella).

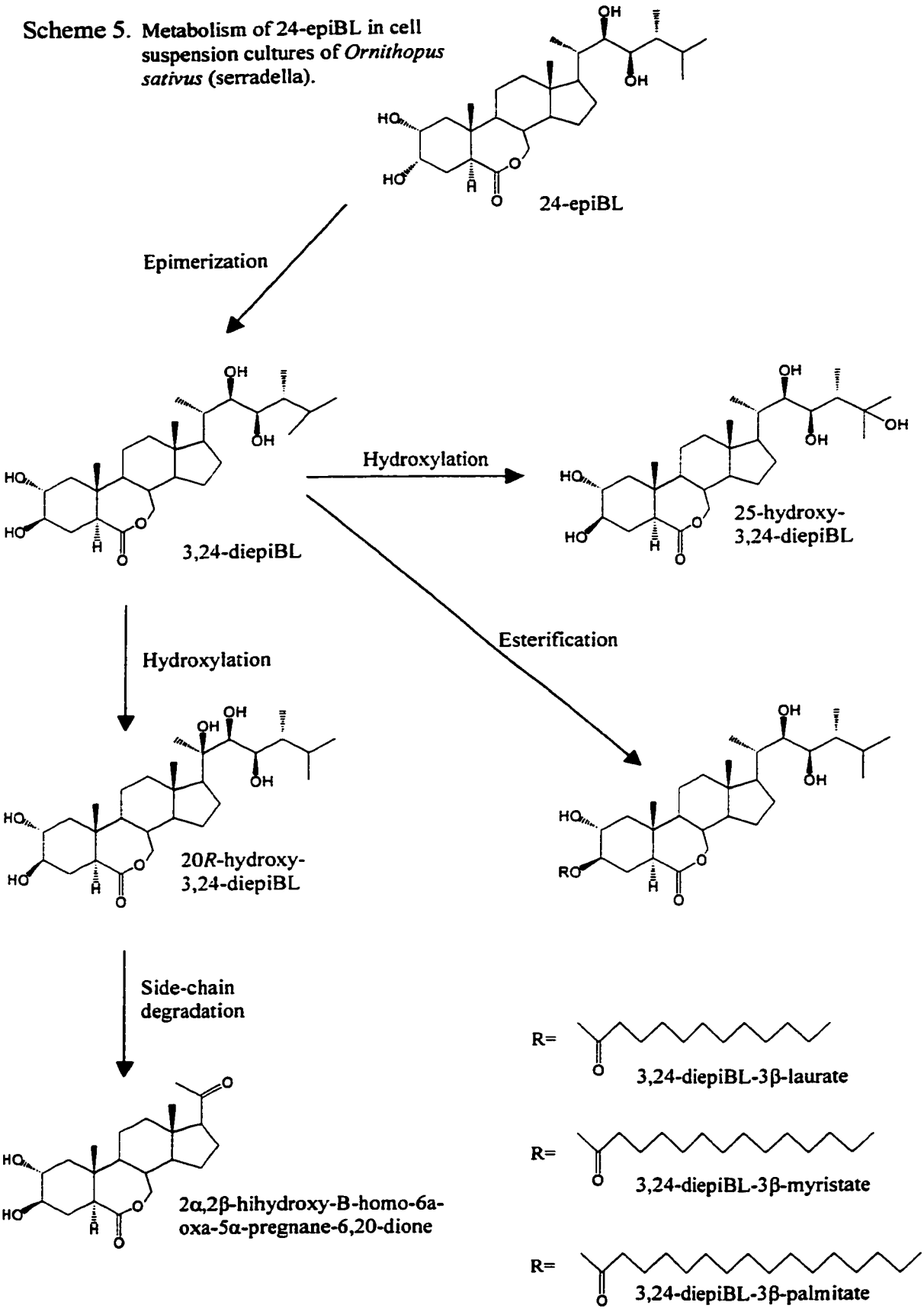

2-*O*-β-D-glucopyranosyl-3,24-diepiCS and 3-*O*-β-D-glucopyranosyl-3,24-diepiCS were also separated from the glycosidic HPLC fractions, and their structures were determined by NMR (Hai et al. 1996). It appears that the 3α-hydroxyl of 24-epiCS is first converted to a 3β-hydroxyl before glycosylation (Scheme 6). Identification of both 3-dehydro-24-epiCS and 3,24-diepiCS indicates that the inversion of configuration at C-3 occurs via an oxidation/reduction mechanism (Hai et al. 1996) opposite to that identified in the conversion of TE to TY (Suzuki et al. 1994 and Griffith et al. 1995). At no time was 24-epiBL identified in cell cultures of *L. esculentum* when feeding experiments were conducted using [^{3}H]-24-epiCS as a precursor.

Tomato cell culture feeding experiments using [^{3}H]-24-epiBL resulted in a number of glycosylated metabolites. Hydroxylation at positions C-25 and C-26 and subsequent glycosylation at these positions, similar to that observed for 24-epiCS, produced both 25-β-D-glucopyranosyloxy-24-epiBL (Schneider et al. 1994) and 26-β-D-glucopyranosyloxy-24-epiBL (Hai et al. 1995) in a ratio of approximately 1:1 (Scheme 7). Other minor glucosidic metabolites in the tomato cell cultures were not further characterized.

The result of later experiments allowed the identification and characterization of the enzymes responsible for the C-25 and C-26 hydroxylation activities. Treatment of tomato cell cultures with the cytochrome P450 mono-oxygenase inhibitors clotrimazole and ketoconazole resulted in a strong decrease in C-25 hydroxylation while C-26 hydroxylation was unaffected (Winter et al. 1997). The results of this study clearly indicate that C-25 and C-26 hydroxylations are catalyzed by two different enzymes and

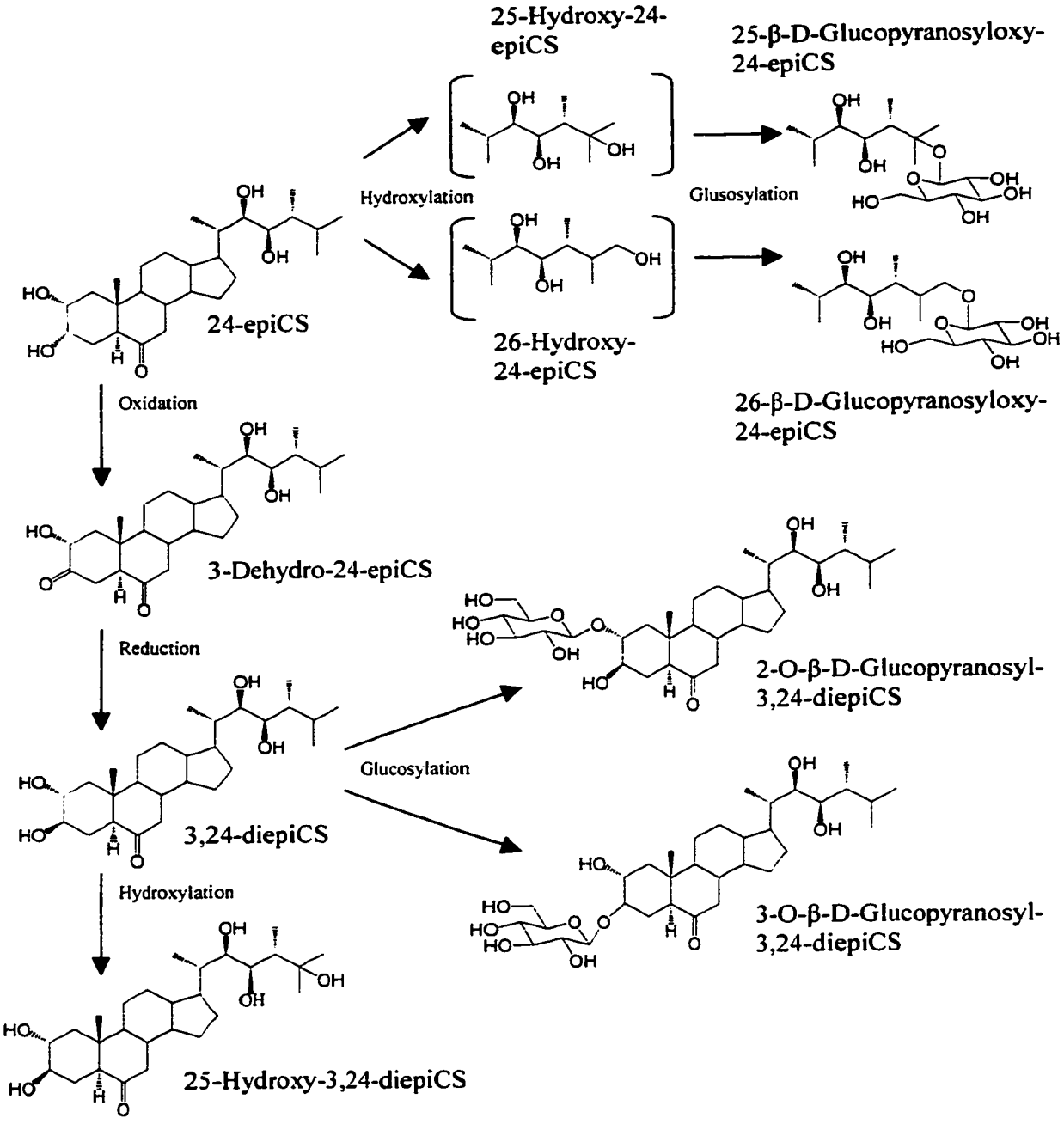

Scheme 6. Metabolism of 24-epiCS in cell suspension cultures of *Lycopersicon esculentum* (tomato).

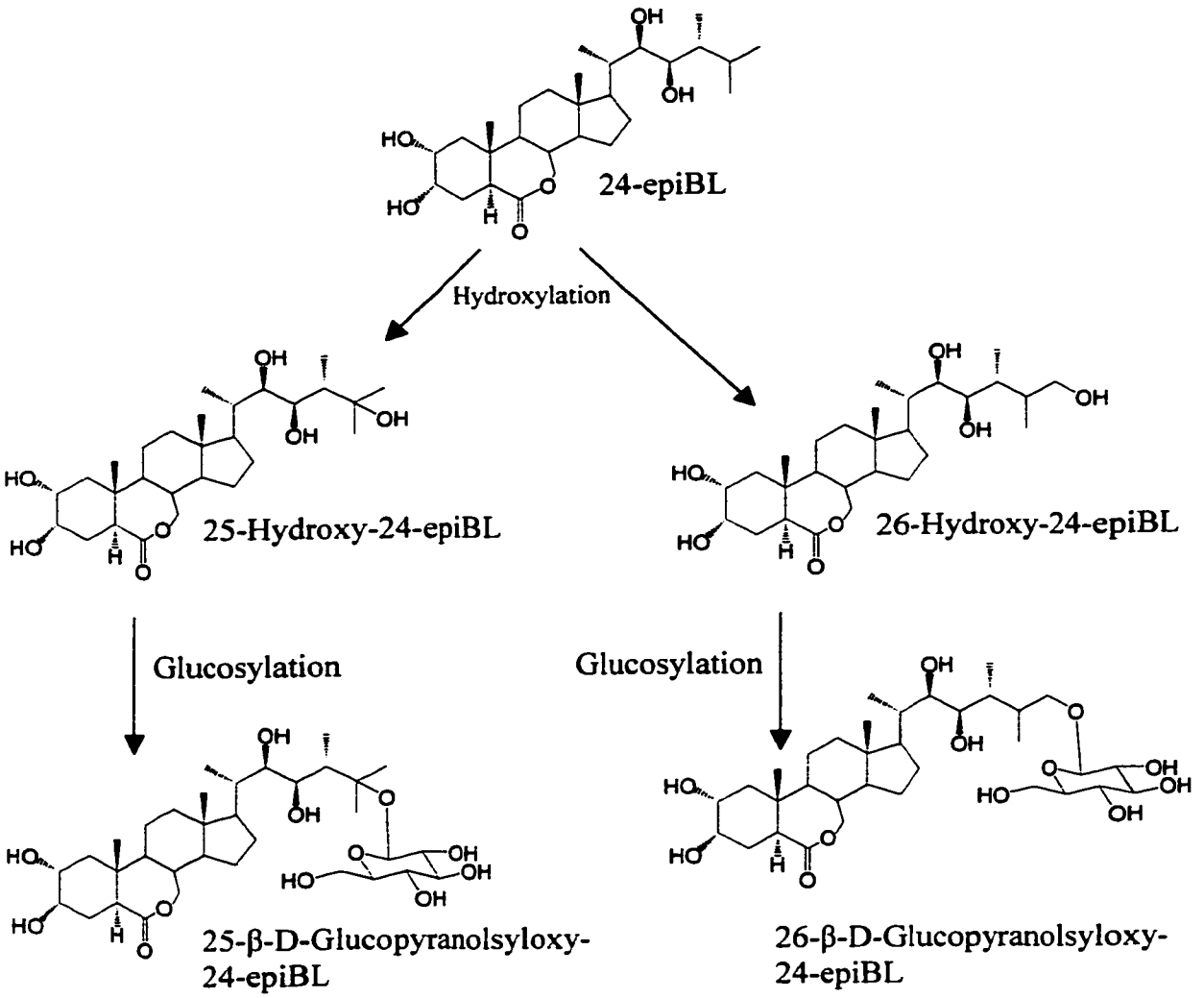

Scheme 7. Metabolism of 24-epiBL in cell suspension cultures of *Lycopersicon esculentum* (tomato).

that the enzyme catalyzing C-26 hydroxylation is not a typical cytochrome P450 mono-oxygenase. When 24-epiBL was added to tomato cell cultures with the common cytochrome P450 inducers, ethanol, $MnCl_2$, phenobarbital, pregnenolone 16α-carbonitrile or clofibrate, hydroxylation at positions C-25 or C-26 was not induced. The substrate analogues (22*S*,23*S*)-20-HomoBL, 24-epiCS, ecdysone and 20-hydroxy-ecdysone also failed to induce hydroxylation at positions C-25 and C-26. Hydroxylation activity could only be induced with either 24-epiBL or BL application. Finally, induction of hydroxylation activity with either 24-epiBL or BL in the presence of the protein synthesis inhibitor cycloheximide, could not be detected. The authors concluded that the increase in both hydroxylase activities is dependent upon gene expression by specific action of the substrates 24-epiBL and BL (Winter et al. 1997).

C MATERIALS AND METHODS

C.1 Molecular Cloning

C.1.1 Plasmid DNA Preparation

Plasmid DNA was prepared (Birnboim and Doly 1979, Ish-Horowicz and Burke 1981) by the centrifugation of 3 ml of overnight-grown *E. coli* bacterial culture for 30 seconds in an Eppendorf microfuge at 13 000 rpm. The supernatant was removed by aspiration and the bacterial pellet was resuspended in 80 µl of 25 mM Tris-HCl, 10 mM EDTA, 1% glucose (w/v), and 5 µl RNase A (10 mg/ml), and chilled on ice for 5 minutes. Then 160 µl of 0.2 N NaOH and 1% SDS (w/v) was added and chilled on ice for 5 minutes, followed by the addition of 120 µl of 3M NaOAc for 5 minutes on ice. The suspension was centrifuged and the supernatant transferred to 360 µl of 7.5 M AmOAc for 15 minutes on ice. The DNA was precipitated with the addition of 0.8 volumes of isopropanol for 10 minutes on ice. After centrifugation the supernatant was removed by aspiration and the pellet washed with 70% EtOH and redissolved in 20 µl of sterile ddH_2O.

All plasmid preparations destined for sequencing were prepared using the Midi-Prep kit (Qiagen) as recommended by the supplier.

DNA templates prepared for sequencing were purified as described above and further processed as follows. A reaction volume of 20 µl was prepared containing 2 µg of double-stranded template DNA and 0.2 M NaOH, and incubated at 25°C for 10 minutes. The appropriate primer was added to a final concentration of 3.6 ng/µl as well as 0.14 M AmOAc. The mixture was precipitated with the addition of 150 µl of 95% EtOH for 30

minutes at -70°C. After centrifugation, the supernatant was removed by aspiration and washed with 70% EtOH. The DNA was resuspended in the T7 DNA polymerase reaction mixture provided by the manufacturer in the sequencing kit (Pharmacia Biotech).

C.1.2 Genomic DNA Preparation

Approximately 3 g of *Arabidopsis* tissue was frozen and pulverized in liquid nitrogen. Initially, 20 ml of Carlson lysis buffer (0.1M Tris-HCl pH9.5, 2% hexadecyltrimethylammonium bromide (CTAB), 1.4 M NaCl, 1% polyethylene glycol 8000, 20 mM ethylenediaminetetraacetic acid, 50µl β-mercaptoethanol/l buffer, 4 mg RNase A/l buffer) prewarmed to 74°C was added and vortexed for 10 seconds. The mixture was incubated at 74°C for 20 minutes, cooled to 25°C, and 20 ml of chloroform/isoamyl alcohol (24:1 $^{v}/_{v}$) was added. The samples were then centrifuged for 10 minutes at 5000xg and the aqueous phase was transferred to 20 ml isopropanol at 25°C for 30 minutes. The sample was again centrifuged for 20 minutes at 12 000xg. The pellet was resuspended in 5 ml of 1M NaCl for 30 minutes at 62°C and then transferred to 3.5 ml of isopropanol. The sample was centrifuged for 10 minutes at 4°C at 12 000xg. The supernatant was discarded and the pellet washed with 70% ethanol. The pellet was allowed to dry at 25°C and then resuspended in 1ml of sterile ddH_2O.

C.1.3 Sequencing of the GBGe166 cDNA

The GBGe166 cDNA (Plant Molecular Biology Laboratory, Grenoble Cedex, France) was sequenced on both strands using a double stranded template by dideoxy

chain termination (Sanger et al. 1977) using the T7 DNA polymerase system (Pharmacia Biotech) and oligonucleotide primers. Analysis of the translated amino acid sequence using the Expert Protein Analysis System(ExPASy,http://www.expasy.ch/tools/dna.htmL) translation tool, provided by the Swiss Institute of Bioinformatics, indicated that the GBGe166 cDNA encoded the complete sequence of *AtST6* cloned into the pBluescript.

C.1.4 Sequencing Gels

The sequencing gels contained either 4% or 5% acrylamide with a ratio of acrylamide to *bis*-acrylamide of 20:1 (w/w) and were made in 2 x TBE buffer containing 8 M urea. The gels were pre-electrophoresed for 30 minutes prior to sample loading. The DNA was denatured at 75°C for 2 minutes and cooled rapidly on ice before loading. The gels were run at 37 W constant power. An average of 450 nucleotides could be resolved per reaction by using a combination of 4% and 5% resolving gels.

C.1.5 Cloning of *AtST4a* and Binary Vector p444 Construction

AtST4a was identified though a BLAST search of The *Arabidopsis* Information Resource (TAIR, http://www.arabidopsis.org) database using *AtST1* as a query sequence.

The oligonucleotides, 5'-GCGGATCCATGGATGAAAAA-3' and 5'-GGGGTACCCTTAATAGATTA-3' were used to amplify the coding sequence of *AtST4a* from 100 ng of *A. thaliana* ecotype Col-0 genomic DNA using PWO DNA Polymerase (Roche Molecular Biochemicals Molecular Biochemicals). The oligonucleotides were designed to introduce a *Bam*HI and a *Kpn*I restriction site at the respective 5' and 3' ends

of the cDNA. The PCR product was digested with *Bam*HI and *Kpn*I, and then ligated to the corresponding sites of the pQE30 polylinker using T4 DNA ligase (New England Biolabs) producing pAtST4a.

The binary vector construct pRD444 was built for *Arabidopsis thaliana* Agrobacterium-mediated vacuum infultration. The oligonucleotides, 5'-CATGCCATGGATGAAAAAGATAGACC -3' and 5'-GCCCTAGGTTAGGAATTTCAAACCGGAAC-3' were used to amplify the coding sequence of *AtST4a* from 1 ng of pAtST4a using PWO DNA Polymerase (Roche Molecular Biochemicals Molecular Biochemicals). The oligonucleotides were designed to introduce *Nco*I and *Bam*HI restriction sites at the respective 5' and 3' ends of the cDNA. The PCR product was digested with *Bam*HI and *Kpn*I, and then ligated to the corresponding sites of the pBI524 (Datla et al. 1993) polylinker using T4 DNA ligase (New England Biolabs). A 2000 base pair fragment was isolated from the intermediate construct upon digestion with *Hind*III and *EcoRI*, containing an enhanced dual minimum 35S promoter, an AMV leader sequence, the in frame *AtST4a* gene and a NOS terminator sequence. This 2 kbp fragment was ligated into the corresponding sites of the pRD400 (Datla et al. 1992) polylinker using T4 DNA ligase (New England Biolabs) producing pRD444. As the cloned *AtST4a* gene would use the supplied translational start codon of the pBI524 plasmid, it was necessary to confirm that *AtST4a* was incorporated in-frame. The oligonucleotide, 5'-GGTAATCTATCTCCCAAGG-3', was developed to sequence the 5' extremity of *AtST4a* beginning approximately 100 nucleotides downstream of the start codon. Dideoxy chain termination was performed in a similar manner as described

previously by the Sheldon Biotechnology Center, McGill University, Montreal. It was determined that the start codon of *AtST4a* was in-frame with the start codon of the pBI524 plasmid.

C.1.6 Cloning of *AtST6*

AtST6 was amplified by PCR using the cDNA GBGe166 as template with Pwo DNA Polymerase (Roche Molecular Biochemicals Molecular Biochemicals). The oligonucleotide primer used for the amplification, 5'-ACATGCATGCATGGAGGCTTCTAAAGAAGC -3' was designed to introduce an *Sph*I restriction site at the 5' end of the cDNA. The second primer, 5'-GTAAAACGACGGCCAGT-3' (M13 -20), included a *Kpn*I restriction site from the pBluescript SK vector (Stratagene) at the 3' end of the cDNA. The PCR product was digested with *Sph*I and *Kpn*I and ligated into the corresponding restriction sites of the pQE30 polylinker (Qiagen) using T4 DNA ligase (New England Biolabs) producing pAtST6.

C.1.7 Restriction Enzyme Digestion and Agarose Gel Electrophoresis

Restriction enzymes were used as recommended by the suppliers. One unit of restriction enzyme was used per microgram of DNA and the reaction was allowed to proceed for three hours at the recommended temperature. At the end of the reaction time, the DNA was loaded directly on the agarose gel for electrophoresis.

Agarose gels were prepared by melting agarose to a concentration of 0.7% to 1.5% in TAE buffer and adding 0.5 µl/ml of ethidium bromide (1µg/ml). The electrophoresis was run at 85 volts and a 1 Kbp or 100 bp ladder was used as molecular weight markers (MBI Fermentas).

DNA fragments for cloning were excised and isolated from agarose gel using the Qiaex II gel extraction kit (Qiagen).

C.1.8 Alignment of Deduced Sequences

The DNA sequences of *AtST4a* and *AtST6* were translated with the Expert Protein Analysis System (ExPASy, http://www.expasy.ch/tools/dna.htmL) translation tool provided by the Swiss Institute of Bioinformatics. Multiple sequence alignments were performed with the ClustalW1.8 program (http://dot.imgen.bcm.tmc.edu:9331/multi-align/multi-align.htmL) provided by the Baylor College of Medicine. Genomic distribution, map locations and the number of *Arabidopsis* ST genes were determined with resources available at the TAIR site. The matrix of amino acid sequence identities between all of the *Arabidopsis* STs and the dendrogram were generated with tools available at the Canadian Bioinformatics Resources web site (www.cbr.nrc.ca)

C.2 Enzymology

C.2.1 Protein Extraction

Overnight bacterial cultures (3mL) consisting of *E. coli* XL1 Blue and recombinant pQE30, grown at 37°C in LB containing tetracycline (100 µg mL^{-1}) and

ampicillin (50 μg mL^{-1}) were used to inoculate 200 mL of the same medium. After 5 hours incubation at 37°C, isopropyl β-D-thiogalactopyranoside (IPTG) was added to a final concentration of 1 mM. Cultures were grown overnight at 18°C and then centrifuged at 5000X*g* for 20 min. Cell pellets were resuspended in 20 mL of buffer A (50 mM sodium phosphate, pH 8.0, 0.3 M NaCl, 14 mM 2-mercaptoethanol) and then lysed by sonication. The lysate was centrifuged at 10 000X*g* for 20 min and the supernatant applied to a nickel-nitrilotriacetic acid (Ni-NTA) agarose column (Qiagen) preequilibriated with buffer A. The column was washed with buffer B (50 mM sodium phosphate, pH 6.0, 0.3 M NaCl, 14 mM 2-mercaptoethanol). The enzyme was eluted from the column with buffer B containing 500 mM imidazole.

C.2.2 Protein Determination and Sulfotransferase Assay

Protein concentration was determined by the method of Bradford using the Bio-Rad dye reagent and bovine serum albumin as the standard protein (Bradford 1976). Enzyme assays were performed as previously described (Varin et al. 1987) using [^{35}S]PAPS as the sulfonate donor (NEN Life Science Products). Enzyme and [^{35}S]PAPS dilutions were made with 50 mM Tris-HCl pH 7.5 or 50 mM phosphate pH 7.5. BRs and other steroids were dissolved in 50% DMSO or methanol. The reaction consisted of 5 μL of PAPS, 5 μL of acceptor substrate and 40 μL of enzyme (~2 μg). The reaction was allowed to proceed for 10 min at 24°C and then stopped by the addition of 20 μL of 2.5% acetic acid. Reaction samples for AtST6 were not further processed. The sulfonated products were transformed to their ion pairs by the addition of 20uL of 0.1M

tetrabutylammonium dihydrogen phosphate. Radiolabelled products were extracted in 250 μL of ethyl acetate and 100 μL of the organic phase was quantified by liquid scintillation counting. Kinetic parameters were determined from double-reciprocal Lineweaver-Burk plots.

C.2.3 Thin Layer Chromatography

Half of the AtST6 reaction samples (32.5 μl) were loaded on cellulose MN 300 TLC plates (Polygram Cell 3000, Macherey-Nagel) and placed in a resolving chamber containing butanol-acetic acid-water (6:2:2 v/v/v) as the solvent phase. The solvent was allowed to chromatograph for 3 hours at which point the TLC plate was removed and dried at RT. After drying, the TLC plate was layered with a X-OMAT AR (Kodak) film in a dark room and allowed to expose for 4 days in a metal cassette at RT. The film was developed using a Kodak X-OMAT 1000A Processor automated developer.

C.2.4 Western Blot Analysis

Protein extracts were separated by SDS-PAGE on a 12% polyacrylamide gel and transferred to nitrocellulose. AtST4a and AtST6 were detected using anti-AtST2 (AtST2 Genbank accession No. T43254) polyclonal antibodies (dilution 1:3000). Goat anti-rabbit secondary antibodies conjugated to alkaline phosphatase (dilution 1:3000; Bio-Rad) were used to detect the primary antibodies. Anti-AtST2 antibodies were raised in rabbits using purified recombinant AtST2 expressed in *E. coli* as the antigen and were

found to cross-react with several recombinant *Arabidopsis* STs including AtST4a and AtST6.

C.3 Molecular Characterization

C.3.1 Plant Material

Seeds of *Arabidopsis thaliana* ecotype Col-0 were sterilized in a 1.5% sodium chlorite, 0.02% SDS solution for 5 min, rinsed 3 times with sterile distilled water and vernalized for 4 days. Seeds were then spread on MS agarose medium (Murashige and Skoog 1962) or sown onto a Pro-Mix-vermiculite-perlite mixture (1:1:1 v/v/v). Plants were grown for 15 days in a growth chamber with a 16 h photoperiod at 22°C. Fifteen-day-old plants were used for induction experiments.

Experiments requiring the treatment of plants with various chemicals were performed with plants grown *in vitro*, by the addition of 1mL of compound to the medium (20 mL). The compound was distributed with gentle agitation. To reduce any additional stress the plants were not removed from the medium. Salicylic acid (SA) pH 7.0 , ethanol (EtOH), methyl jasmonate (MeJA), NaCl, gibberellic acid (GA), abscisic acid (ABA), zeatin and indole acetic acid (IAA) were added as 20X concentrated stocks. Other plants were subjected to wounding, fungal infection, cold (4°C for 12 or 24h) and heat shock (37°C for 1h), dark, long and short UV irradiation (1h) and flooding. Samples were collected at 12 and 24h intervals and total RNA was extracted immediately.

Fifteen-day-old plants were dissected to isolate tissue from stem, rosette, roots and siliques. A separate group of plants was grown as stated above to isolate flower tissue.

C.3.2 Reverse-Transcription PCR Analysis of *AtST4a* and *AtST6* Expression

The synthesis of cDNA was according to the recommendations of New England Biolabs. Reverse transcription (RT) product was produced by first treating 2.5 μg of total RNA with 20U of DNaseI (Roche Molecular Biochemicals Molecular Biochemicals) in 0.1M Sodium acetate, 5 mM $MgSO_4$ pH 5.0 at 37°C for 10 min. DNaseI was inactivated at 95°C for 5 min, and the RNA was precipitated overnight. The RNA was resuspended in 0.1% diethyl pyrocarbonate (DEPC) treated water and 1.2 μg of oligodT was added. The mixture was heated to 70°C and let cool to room temperature. A reaction cocktail was added to a final concentration of 50U Moloney murine leukemia virus reverse transcriptase (New England Biolabs), 1X reverse transcriptase Buffer (New England Biolabs), 250 μM dNTPs, 24U RNase inhibitor (Roche Molecular Biochemicals), and 0.6 mM bovine serum albumin. The reaction was allowed to proceed for 90 min at 37°C and then heat inactivated for 25 min at 65°C. Gene specific primers were designed and tested against 7 different *Arabidopsis* ST genes to ensure specificity. PCR analysis was performed using the gene specific primers, Ex-Taq DNA polymerase (PanVera) and 2μL of reverse-transcription (RT) product. Control PCR reactions were performed with RT-product, and 100 ng of *A. thaliana* ecotype Col-0 DNA using the actin (ACT1, GenBank accession number U39449) primers, 5'GCTGATGGTGAAGACATTCAAC and 5'CATACATAGCAGGGGCATAAG. The primers were designed within the regions

flanking the actin genes single intron of approximately 100 bp, and could be used to monitor genomic DNA contamination. Actin controls also confirmed that similar quantities of RT-product were present in each reaction.

C.3.3 Vacuum Infiltration of *Arabidopsis thaliana* ecotype Col-0

Arabidopsis thaliana ecotype Col-0 influorescences were allowed to grow to approximately 5 cm high and were decapitated at their base (Benchtold et al. 1993). After 5 days of growth, the plants carefully were removed from soil and their newly emerging secondary influorescence were submerged in an infiltration medium (2.15 g/l MS salts, 1 x B5 vitamins, 5% sucrose, 0.5 g/l MES, 10 pg/ml BA, 0.02% SILWET, pH 5.7) containing the Agrobacterium strain, GV3101 pmp 90 transformed with pRD444 (at an OD_{600} of 0.8) for 1 minute under 25 inches Hg of vacuum pressure. After infiltration the excess Agrobacterium infiltration medium was allowed to drain from the plants. The plants were potted in sterilized soil containing Pro-Mix-vermiculite-perlite (1:1:1 v/v/v), covered with plastic wrap for 2 days and grown in a growth chamber with a 16 hour photoperiod at 23°C. The infiltrated plants were fertilized every 2 weeks with 20:20:20 and grown until seed set. The seeds were collected manually from dry plants, sterilized and vernalized. The seeds were sown on media containing 3% sucrose, 1x B vitamins, 0.43% MS salts, 0.7% phytagar and 50 μg/ml kanamicin at pH 5.7 for 2 weeks, to select for transformants. Resistant individuals were transferred to sterilized soil containing Pro-Mix-vermiculite-perlite (1:1:1 $^{v}/_{v}$), covered with plastic wrap for 2 days and grown with a 16 hour photoperiod at 25°C until seed set.

D RESULTS

D.1 Molecular Cloning

D.1.1 Characterization of *AtST4a* and *AtST6* Clones

Two clones designated p*AtST4a* and p*AtST6*, were isolated and identified by PCR amplification with gene specific primers and restriction digestion. Recombinant AtST4a and AtST6 were expressed in *E. coli* XL1 Blue. Ni-NTA column-purified proteins were prepared and electrophoriesed on a polyacrylamide gel (Figure 5, A and C). Western blot analysis of the lysate from *E. coli* strains carrying the two recombinant plasmids, utilizing anti-AtST2 polyclonal antibodies, confirmed the presence of ST proteins (Figure 5, B and D). The antibodies reacted with a protein band from the lysate with estimated molecular masses of 41.6 and 39.8 KDa for AtST4a and AtST6, respectively. Both, AtST4a and AtST6, exhibit the appropriate molecular mass of the recombinant proteins, including 12 additional amino acid residues contributed by the vector.

D.1.2 Molecular Characterization of *AtST4a*

AtST4a, Genbank accession number is AC005396, is localized to chromosome II spanning nucleotides 38691 to 39728, and is near the genetic marker mi398. *AtST4a* is not in close proximity to any other sulfotransferase genes.

The *AtST4a* deduced protein sequence contains all the amino acids involved in PAPS binding and catalysis as previously described (Marsolais et al. 1995, Marsolais and Varin 1997), and is presented in Figure 6. An amino acid alignment between AtST1 and AtST4a indicates a 42% sequence identity, with a majority of the divergent amino acids being present in a region believed to define substrate specificity (Varin et al. 1995),

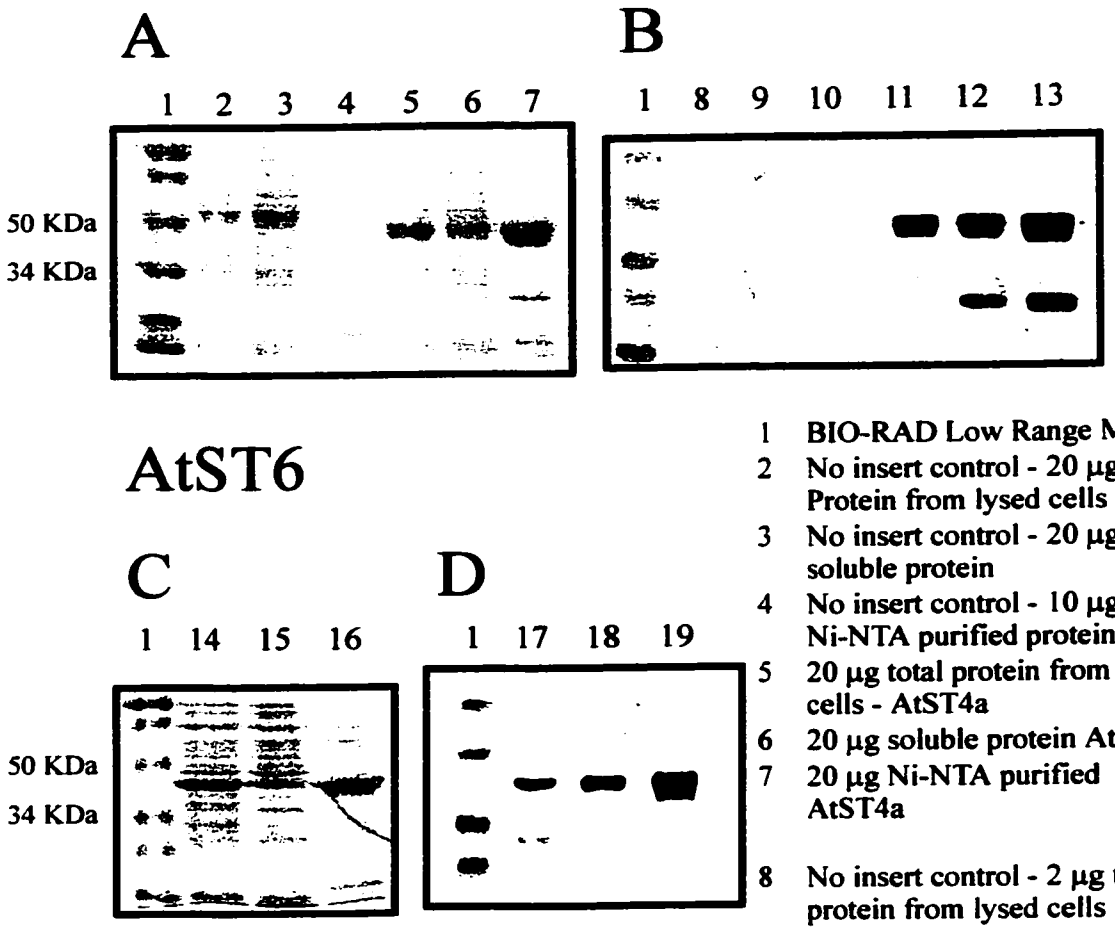

1 BIO-RAD Low Range Markers
2 No insert control - 20 µg total Protein from lysed cells
3 No insert control - 20 µg soluble protein
4 No insert control - 10 µg Ni-NTA purified protein
5 20 µg total protein from lysed cells - AtST4a
6 20 µg soluble protein AtST4a
7 20 µg Ni-NTA purified AtST4a
8 No insert control - 2 µg total protein from lysed cells
9 No insert control - 2 µg soluble protein
10 No insert control - 1 µg Ni-NTA purified protein
11 2 µg total protein from lysed cells - AtST4a
12 2 µg soluble protein AtST4a
13 2 µg Ni-NTA purified AtST4a
14 10 µg total protein from lysed cells - AtST6
15 10 µg soluble protein AtST6
16 7 µg Ni-NTA purified AtST6
17 1 µg total protein from lysed cells - AtST6
18 1 µg soluble protein AtST6
19 1 µg Ni-NTA purified AtST6

Figure 5. SDS-PAGE and Western analysis of AtST4a (A and B) and AtST6 (C and D) recombinant protein production in *E. coli*. Gels designated A are SDS-PAGE and gels designated B are Westerns. Numbers indicate well position. Quantity and protein samples are indicated next to the well number designation. The no insert control is composed of the pQE30 vector without insert, transformed into *E. coli*.

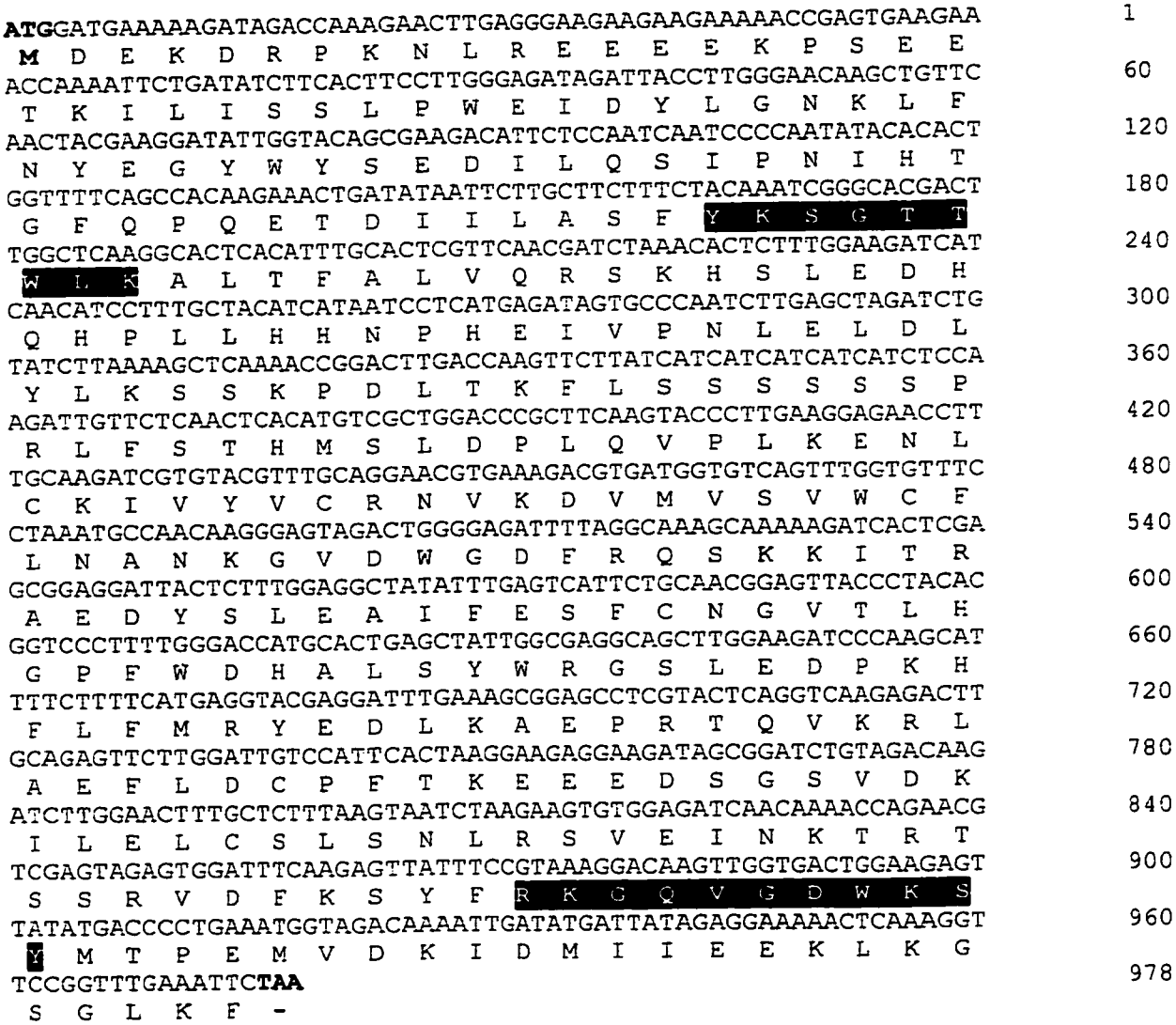

Figure 6. Nucleotide and deduced amino acid sequence of *AtST4a*. Start and stop codons are bolded. Conserved regions I and IV are highlighted in black.

suggesting AtST1 and AtST4a exhibit different substrate specificities. AtST4a and BnST3 alignments are comparable to those obtained between AtST4a and AtST1 with a sequence identity of 43%. AtST4a shares its highest amino acid sequence identities (72% and 85%) with AtST4b and AtST4c, putative BR sulfotransferases. In general, the amino acids that interact with the sulfonate acceptor in AtST4a differ from those of other plant BR STs as determined by residues previously identified in the mouse estrogen sulfotransferase crystal structure. AtST4a shares 39% sequence identities with the flavonol STs of *Flaveria* species and approximately 25% identity with mammalian STs.

D.1.3 Molecular Characterization of *AtST6*

AtST6, Genbank accession number is AC006836, is localized to chromosome II, spanning nucleotides 69115 to 70164, and is positioned near the genetic marker mi320. *AtST6* is a member of the only ST cluster to contain three genes, which also includes *AtST1* and *AtST8*. The composition of this cluster is similar to that of the others. *AtST6* shows a slight relation to both, *AtST1* and *AtST8*, as seen in the dendrogram (Section B.2.2) and exhibits sequence identities of 41% and 45 % with *AtST1* and *AtST8*, respectively. The deduced protein sequence of AtST6 contains all the amino acids involved in PAPS binding and catalysis as previously described (Marsolais et al. 1995, Marsolais and Varin 1997), and is presented in Figure 7.

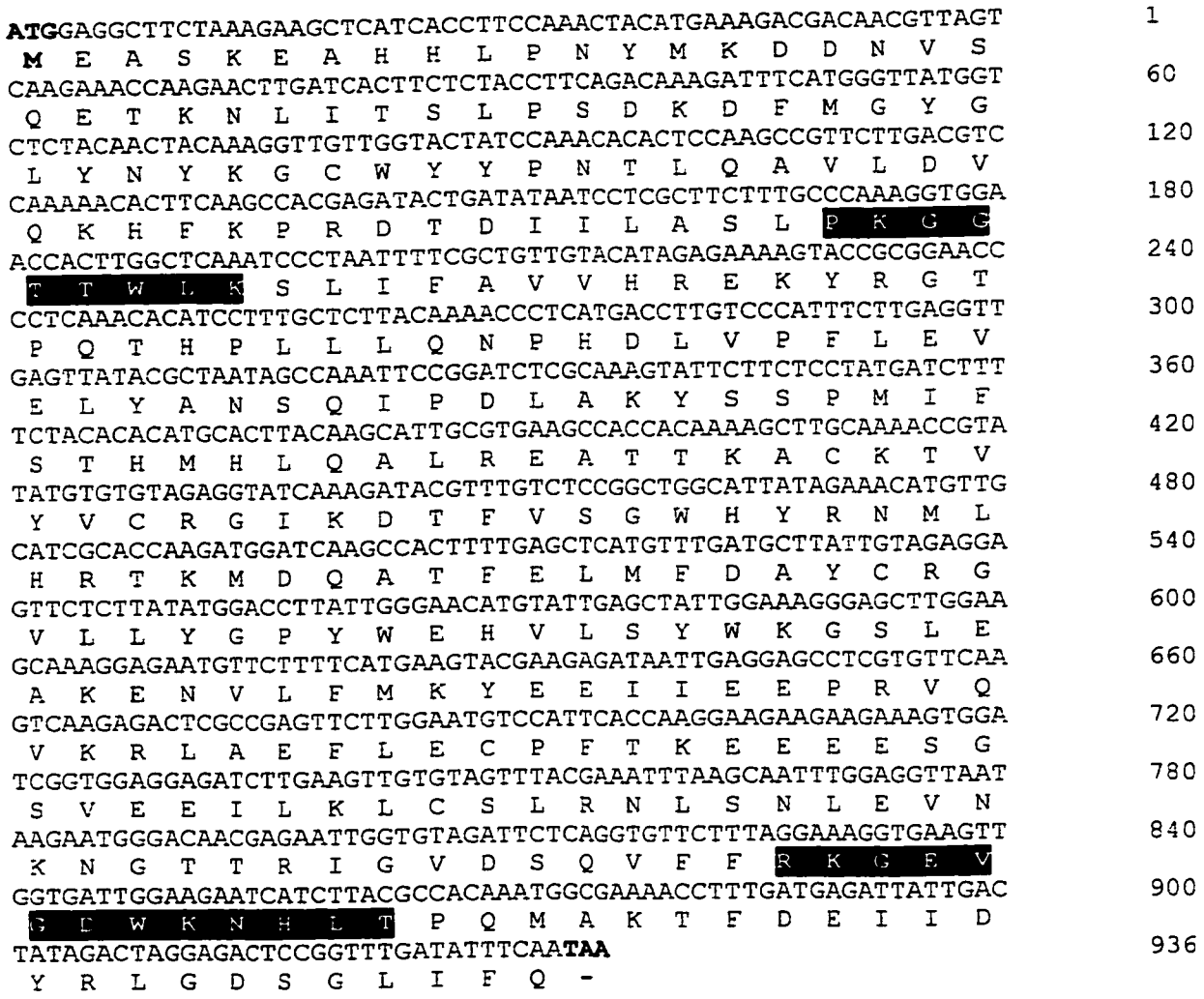

Figure 7. Nucleotide and deduced amino acid sequence of *AtST6*. Start and stop codons are bolded. Conserved regions I and IV are highlighted in black.

D.1.4 RT-PCR Analysis of *AtST4a* and *AtST6* Gene Expression

RT-PCR analysis (Figure 10) failed to identify conditions under which *AtST4a* gene expression was induced. Similarily, RT-PCR analysis (Figure 11) of *AtST6* was unsuccessful in determining conditions for gene expression. Actin control and primer control gels are presented in Figure 8 and 9, respectively.

D.2 Enzymology of the Sulfonation Reaction

D.2.1 Biochemical Characterization of AtST4a

A substrate screen of AtST4a was carried out with a library of compounds including flavonols, phenolic acids, coumarins, glucosinolates, phytosterols, triterpenes, indole acetic acid, zeatin, mammalian-specific steroids, ecdysteroids, catecholamine neurotransmitters, as well as late intermediates and endproducts of the BR pathway, with assay concentrations ranging from 1 to 100 μM. It was determined that AtST4a displayed exclusive specificity for the various forms of BL and its immediate precursors (Table 3). Of all the BRs tested, AtST4a exhibits the highest affinity for (22*R*, 23*R*)-28-homoBL, with an apparent K_m of 19.2 μM and a V_{max} of 34 pkatal mg^{-1} (Table 4). The apparent K_m value for PAPS was found to be 0.4 μM with a V_{max} of 3.8 pkatal mg^{-1}. The catalytic efficiency (V_{max}/K_m) of the enzyme is 6.6-fold higher for (22*R*, 23*R*)-28-HomoBL as compared to BL. The enzyme does not appear to be sensitive to the oxidation state of the B ring, given that 6-deoxo-24-epiCS was accepted with greater affinity than either BL or CS. AtST4a exhibits no activity with the synthetic BRs, (22*S*, 23*S*)-28-HomoBL nor (22*S*, 23*S*)-28-HomoCS at a concentration of 5μM and displays very poor affinity at

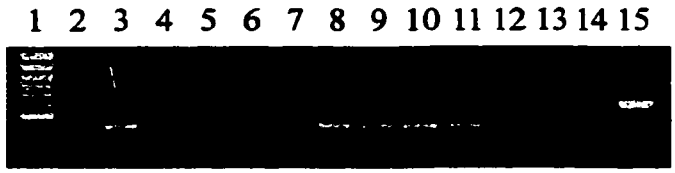

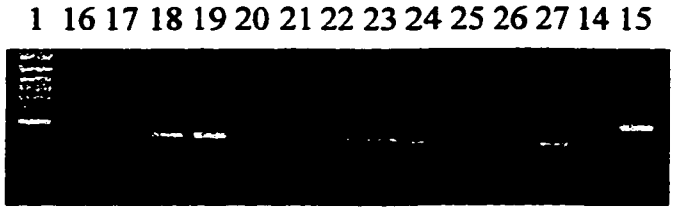

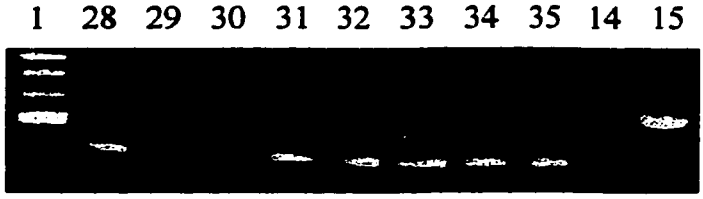

1 MBI Fermentas 100 bp ladder
2 Whole Plant
3 Stem
4 Rosette
5 5 mM Salicylic Acid 24 hrs.
6 Wounding 12 hrs.
7 Wounding 24 hrs.
8 Fungal Infection
9 Cold (4 deg. C) 6 hrs.
10 Heat (40 deg. C) 12 hrs.
11 Heat (40 deg. C) 24 hrs.
12 Etiolation 48 hrs.
13 1 hr. UV-short wave 12 hrs.
14 Negative Control - No template
15 Positive Control - genomic DNA

16 1 hr. UV-long wave 12 hrs.
17 1 hr. UV-long wave 24 hrs.
18 Flooding 12 hrs.
19 Flooding 24 hrs.
20 10 µl Methyl Jasmonate 12 hrs.
21 200 mM NaCl 12 hrs.
22 50 µM Gibberellic Acid 12 hrs.
23 50 µM Gibberellic Acid 24 hrs.
24 50 µM Zeatin 24 hrs.
25 50 µM Indole Acetic Acid 12 hrs.
26 Whole Plant + Flowers
27 Flowers + Siliques

28 1 µM CS 12 hrs.
29 0.1 µM CS 12 hrs.
30 0.01 µM CS 12 hrs.
31 No treatment 12 hrs.
32 1 µM CS 24 hrs.
33 0.1 µM CS 24 hrs.
34 0.01 µM CS 24 hrs.
35 No treatment 24 hrs.

Figure 8. Reverse-transcription PCR testing for genomic DNA contamination by using actin (ACT1) gene specific primers. cDNA samples are indicated beside column numbers. Column 1 is MBI Fermentas 100 bp ladder. Column 14 is a negative control lacking template DNA. Column 15 is a positive control using 100 ng of *Arabidopsis thaliana* genomic DNA.

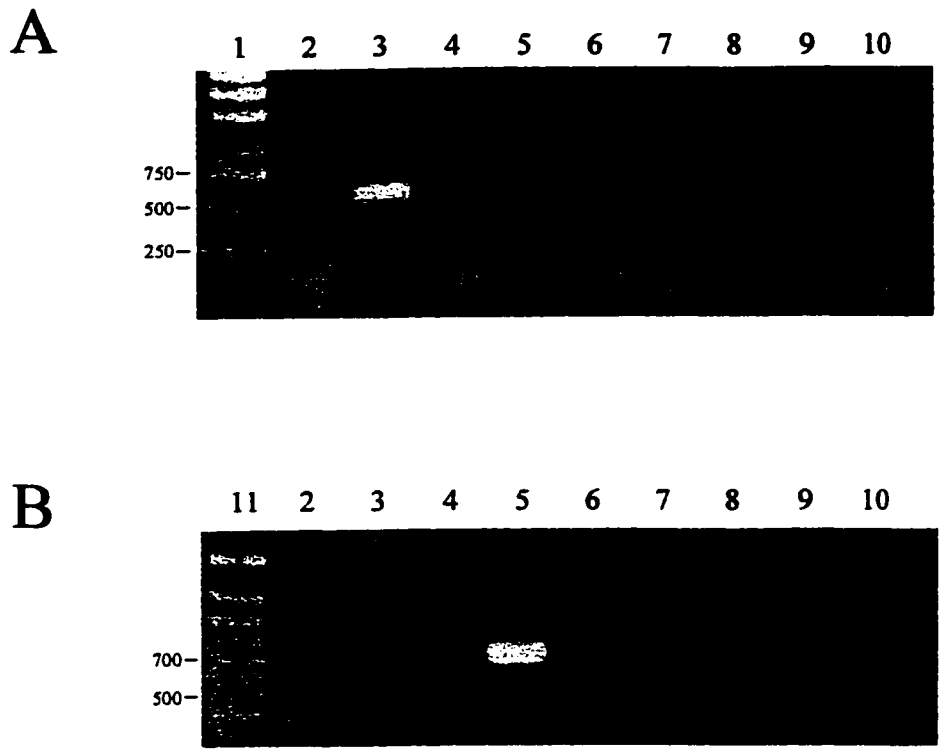

1 MBI Fermentas 1 Kbp ladder
2 p*AtST3c*
3 p*AtST4a*
4 p*AtST3a*
5 p*AtST6*
6 p*AtST5a*
7 p*AtST1*
8 p*AtST7*
9 p*AtST2a*
10 Negative control

11 MBI Fermentas 100 bp ladder plus

Figure 9. Oligonucleotide primer control experiment to ensure gene specific amplification during RT-PCR expression studies. Gel A samples were amplified with *AtST4a* specific primers. Gel B samples were amplified with *AtST6* specific primers. Numbers indicate well position. The template DNA used for each PCR reaction is indicated next to the well designation. Negative controls are PCR reactions without template DNA.

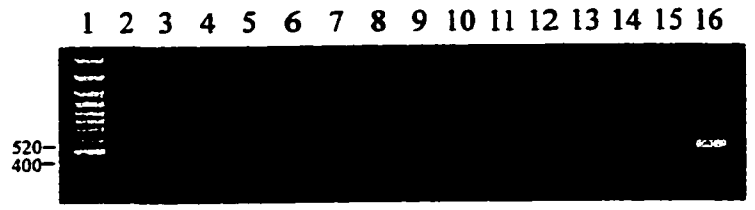

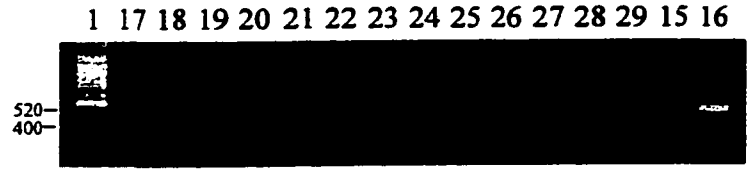

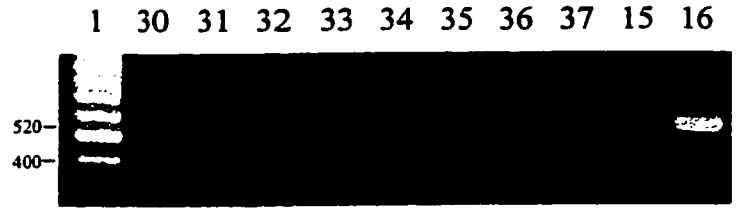

1 MBI Fermentas 100 bp ladder plus
2 Whole Plant
3 Stem
4 Rosette
5 5 mM Salicylic Acid 24 hrs.
6 Wounding 12 hrs.
7 Wounding 24 hrs.
8 Fungal Infection
9 5% EtOH 12 hrs.
10 Cold (4 deg. C) 6 hrs.
11 Heat (40 deg. C) 12 hrs.
12 Heat (40 deg. C) 24 hrs.
13 Etiolation 48 hrs.
14 1 hr. UV-short wave 12 hrs.
15 Negative Control - No template
16 Positive Control - genomic DNA

17 1 hr. UV-long wave 12 hrs.
18 1 hr. UV-long wave 24 hrs.
19 Flooding 12 hrs.
20 Flooding 24 hrs.
21 10 µl Methyl Jasmonate 12 hrs.
22 200 mM NaCl 12 hrs.
23 50 µM Gibberellic Acid 12 hrs.
24 50 µM Gibberellic Acid 24 hrs.
25 50 µM Abscisic Acid 12 hrs.
26 50 µM Zeatin 24 hrs.
27 50 µM Indole Acetic Acid 12 hrs.
28 Whole Plant + Flowers
29 Flowers + Siliques

30 1 µM CS 12 hrs.
31 0.1 µM CS 12 hrs.
32 0.01 µM CS 12 hrs.
33 No treatment 12 hrs.
34 1 µM CS 24 hrs.
35 0.1 µM CS 24 hrs.
36 0.01 µM CS 24 hrs.
37 No treatment 24 hrs.

Figure 10. RT-PCR analysis of *AtST4a* expression. Reactions run on 1.5% agarose gels. Numbers indicate well position. Growth conditions are indicated next to the well numbers.

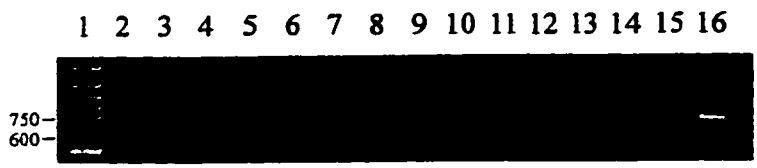

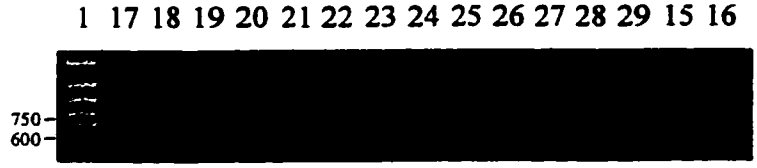

1 MBI Fermentas 100 bp ladder plus
2 Whole Plant
3 Stem
4 Rosette
5 5 mM Salicylic Acid 24 hrs.
6 Wounding 12 hrs.
7 Wounding 24 hrs.
8 Fungal Infection
9 5% EtOH 12 hrs.
10 Cold (4 deg. C) 6 hrs.
11 Heat (40 deg. C) 12 hrs.
12 Heat (40 deg. C) 24 hrs.
13 Etiolation 48 hrs.
14 1 hr. UV-short wave 12 hrs.
15 Negative Control - No template
16 Positive Control - genomic DNA

17 1 hr. UV-long wave 12 hrs.
18 1 hr. UV-long wave 24 hrs.
19 Flooding 12 hrs.
20 Flooding 24 hrs.
21 10 µl Methyl Jasmonate 12 hrs.
22 200 mM NaCl 12 hrs.
23 50 µM Gibberellic Acid 12 hrs.
24 50 µM Gibberellic Acid 24 hrs.
25 50 µM Abscisic Acid 12 hrs.
26 50 µM Zeatin 24 hrs.
27 50 µM Indole Acetic Acid 12 hrs.
28 Whole Plant + Flowers
29 Flowers + Siliques

Figure 11. RT-PCR analysis of *AtST6* expression. Reactions run on 1.5% agarose gels. Numbers indicate well position. Growth conditions are indicated next to the well numbers.

TABLE 3

Substrate specificity of recombinant AtST4a

Substrate [a]	Relative activity in % at 200 μM	Relative activity in % at 5 μM
Brassinolide	22	28
Castasterone	31	33
24-Epibrassinolide	50	26
24-Epicastasterone	12	17
(22*R*, 23*R*)-28-Homobrassinolide [b]	100	97
(22*R*, 23*R*)-28-Homocastasterone [c]	27	100
(22*S*, 23*S*)-28-Homobrassinolide	10	5
6-deoxo-24-Epicastasterone	7	17
22,23,24-Trisepibrassinolide	15	5
22,23,24-Trisepicastasterone	14	5

[a] Substrates with relative activities of <10% are not included.

[b] Maximun specific activity equals 22 pkatal mg^{-1}.

[c] Maximun specific activity equals 15 pkatal mg^{-1}.

TABLE 4

Kinetic parameters of recombinant AtST4a for the preferred substrates

Substrate	K_m (μM)	V_{max} (pkatal mg^{-1})	V_{max}/K_m (pkatal mg^{-1} μM^{-1})
Brassinolide	16	5	0.3
Castasterone	14	3	0.2
24-Epibrassinolide	43	10	0.2
24-Epicastasterone	4	0.6	0.2
(22R, 23R)-28-Homobrassinolide	19	34	1.8
(22R, 23R)-28-Homocastasterone	7	9	1.3
6-deoxo-24-Epicastasterone	5	2	0.4

200 μM. AtST4a did not accept any other BR intermediates. Contrary to AtST1, AtST4a displayed no activity when tested with mammalian specific steroids.

D.2.2 Biochemical Characterization of AtST6

AtST6 was also screened against a library of substrates. AtST6 displayed activity with common alcohols as well as plant-specific alcohols including methanol, ethanol, isopropanol, butanol and *cis*-3-hexen-1-ol (Figure 13), as determined by preliminary thin-layer chromatography experiments. All alcohols were tested at concentrations of 0.02, 0.2 and 2% (v/v) of alcohol substrate per reaction. Methanol was accepted in a dose dependant manner as product formation decreases with decreasing substrate concentration indicating a higher K_m. Ethanol sulfonate product formation decreased with decreasing substrate concentration, as seen with methanol. This would indicate that AtST6 has less affinity for this alcohol as compared to other substrates. There did not appear to be variation in product formation over the concentration range tested for isopropanol. Both butanol and *cis*-3-hexen-1-ol produced equivalent amounts of products over the range of concentrations tested. Butanol appeared to be accepted with greater affinity than *cis*-3-hexen-1-ol. The TLC data indicates that butanol was accepted with greatest efficiency followed by isopropanol, ethanol, *cis*-3-hexen-1ol and then methanol. The natural alcohol, 2-ketol linolenic acid, was not accepted. Kinetic parameters have not been determined for AtST6 at this writing.

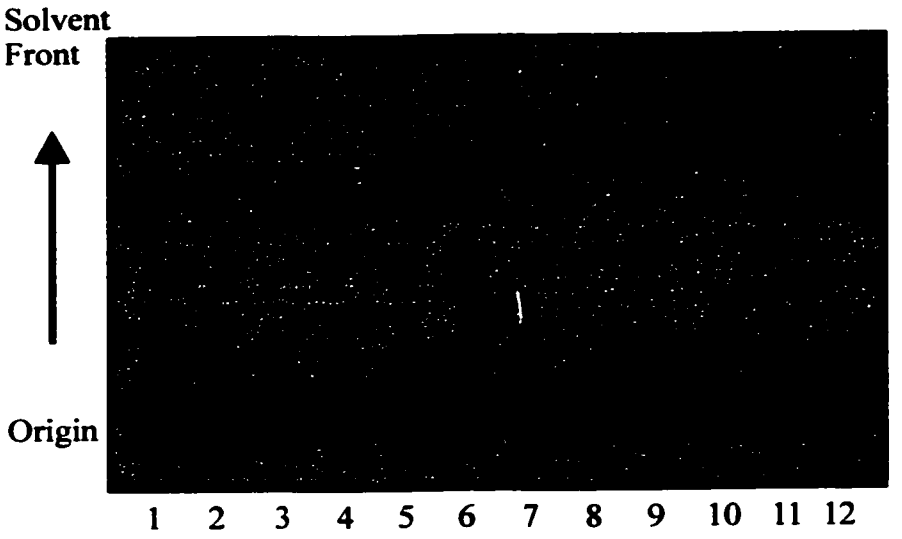

1 2% MeOH
2 0.2% MeOH
3 0.02% MeOH

4 2% EtOH
5 0.2% EtOH
6 0.02% EtOH

7 2% IPA
8 0.2% IPA
9 0.02% IPA

10 2% BuOH
11 0.2% BuOH
12 0.02% BuOH

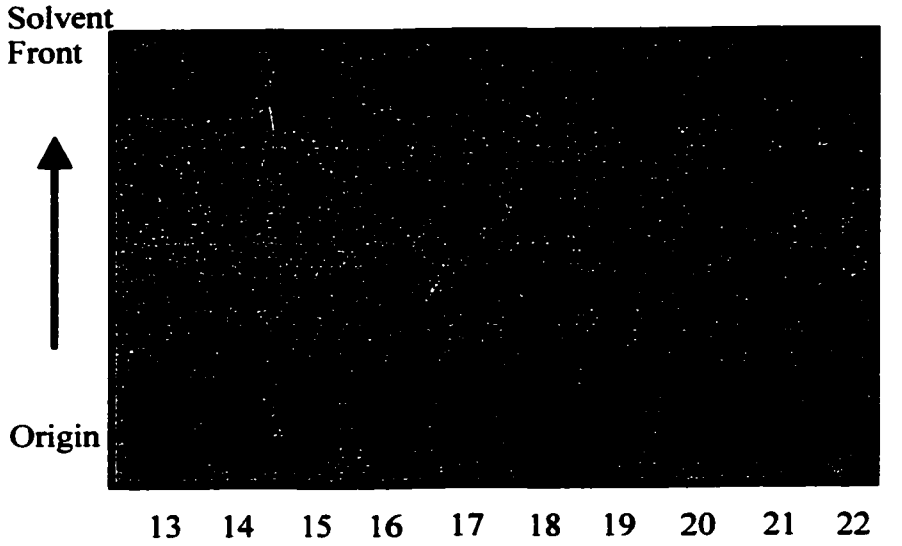

13 2% cis-3-hexen-1-ol
14 0.2% hexen
15 0.02% hexen

16 2% 2-ketol linolenic acid
17 0.2% 2-ketol
18 0.02% 2-ketol

19 ddH_2O
20 50 mM Tris-HCl
21 50 mM Phosphate
22 PAPS

Figure 12. Recombinant AtST6 catalyzed reactions run on TLC. The reactions consisted of 2 μg of AtST6, 2 μM PAPS and 2%, 0.2% or 0.02% (v/v) substrate. Control reactions are shown in lanes 19 to 22 were these compounds were substituted for substrate. Reactions were allowed to proceed for 25 minutes at 25 degrees C. 30% of the reaction volume was loaded on the TLC. The solvent phase was composed of BAW. Product is indicated by the arrows.

D.3 Transgenic *Arabidopsis thaliana* Analysis

D.3.1 T-DNA Copy Number and AtST4a Production

Vacuum-infultration and *in vitro* screening of infiltrated seeds on kanamycin growth medium generated 12 putative transformed T_1 lines. Due to the fragility of the putative transgenic lines, it was impossible to collect tissue samples without destroying the plants, therefore, none were harvested in order to ensure propagation of the plant lines. As no tissue samples were taken, T-DNA copy number was not determined through genomic DNA analysis. Similarly, it was impossible to determine whether AtST4a was produced *in vivo* without Western analysis of the tissue samples. This work will be performed on T2 generation plants.

D.3.2 Phenotypic Analysis of Putative Transgenic *Arabidopsis thaliana*

The 12 putative transgenic *Arabidopsis* lines presented phenotypes ranging from wild-type-like to dwarf as well as an intermediate, "slender" phenotype. Examples of each phenotype, wild-type, wild-type-like, slender and dwarf are presented in Figure 14.

Wild-type

Line 17 presented wild-type characteristics. At maturity it possessed 4 bolts (~35 cm heigh), a normal-size rosette (~8 cm diameter) and a large number of normal flowers, which all produced siliques and seeds.

Lines 13-1, 13-2, 14-1 and 23, likewise presented a wild-type phenotype with a few exceptions. All individuals displayed an abnormal senesence pattern, where part of

the plant was dead and drying while the remainder produced fresh growth. Furthermore, many of the flowers displayed an abnormal morphology. These abnormal flowers produced irregular siliques that aborted early in development and did not set seed. Approximately 10% of the siliques were aborted in lines 14-1 and 23, where as 30-40% of the siliques were aborted in lines 13-1 and 13-2. It is likely that 13-1 and 13-2 are clonally related, originating from the same transformation event, as each line originated from the same plant and displays a similar phenotype.

Slender

The two lines, 7-1 and 7-2, produced mature plants that had a rosette one-fourth the diameter (~2 cm) of a wild-type plant, and a single slender bolt approximately one-third (~10 cm) the height of a wild-type plant. Line 7-1 flowered very early and eventually produced two siliques containing seeds. Line 7-2 produced five small, abnormal flowers and all lead to aborted siliques. It is likely that 7-1 and 7-2 are clonally related, as each line originated from the same vacuum infiltrated mother plant.

Line 37 produced a phenotype similar to 7-1, however, it had 4 slender bolts exhibiting a total of 53 flowers. Only 17 siliques were produced which set seeds, all others shared an abnormal, hooked phenotype and aborted early in development.

Dwarf

Line 27 showed a dwarf phenotype for much of its lifetime, with a small rosette and no visible bolt. Later it formed 3 bolts which produced 31 flowers, many of which

were abnormal. Only 8 siliques were formed which produced seeds, the rest were aborted.

Lines 12 and 14-2 presented a dwarf phenotype for much of their life. Both eventually formed a single slender bolt of about 12 cm and then died. Due to the severe phenotype of 14-2 and the wild-type phenotype of 14-1, it is unlikely that they are clonally related even though they originated from the same infiltrated mother plant.

Lines 8 and 15 displayed the most extreme phenotype of all the putative transgenic lines. Each presented a dwarf phenotype similar to that of line 27. However, neither line formed a bolt and each died early in soil.

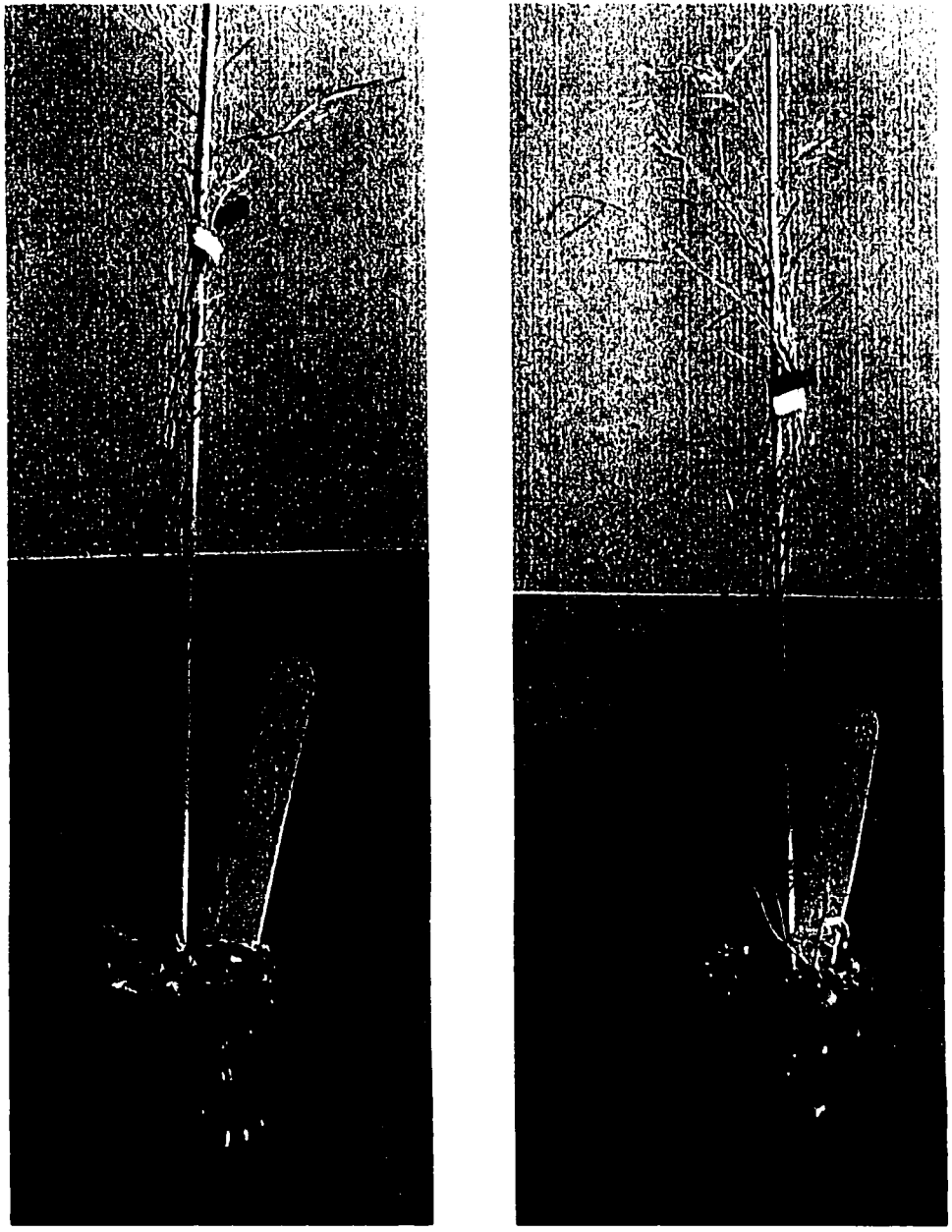

Figure 13. Photos of 7 week old *Arabidopsis thaliana* plants. The wild-type plant spent 2 weeks in solid medium without selection. The putative transgenic lines spent 2 weeks in solid medium in the presence of 50 µg/ml kanamycin. From left to right: wild-type - #2, wild-type - line 13-2, slender - line 7-2 and dwarf - line 27.

E DISCUSSION

E.1 *AtST4a*

E.1.1 Molecular Characteristics

RT-PCR studies of *AtST4a* expression were not successful in determining induction conditions. Expression of the *CPD* gene, encoding a 23α-hydroxylase that catalyzes a step in BR biosynthesis (Szekeres et al. 1996), is limited to the cotyledons and leaf primordia of seedlings along with the adaxial parenchyma of expanded leaves in light-grown plants. Given that *CPD* expression is strictly limited to specific tissues, it is likely that BRs are synthesized locally followed by transportation to their site of action. It is, therefore, possible that *AtST4a*, a BR-modifying enzyme, is likewise localized to the same tissues. Given that mRNA extracts were performed on whole plant tissues, a dilution effect of the mRNA transcript may account for the apparent lack of expression. Alternatively, as a BR-modifying enzyme, it may be temporally regulated to periods of intensive growth or senescence. Nevertheless, the possibility still remains that *AtST4a* is expressed at very low levels. Expression studies utilizing transgenic plants containing the *AtST4a* promoter fused to a reporter gene would be the most powerful tool to accurately and quickly determine the expression pattern of *AtST4a*.

E.1.2 Enzymology of Brassinosteroid Sulfonation

AtST1 displays 87% amino acid identity with BnST3. Both enzymes exhibit greatest affinity for 24-epicathasterone as substrate with similar kinetic parameters, in addition to a similar induction pattern (Rouleau et al. 1999). It is clear that AtST1 and

BnST3 are homologous proteins from *Arabidopsis thaliana* and *Brassica napus*, respectively, and likely serve similar functions in these species.

Strikingly, AtST1 and AtST4a have an amino acid identity of only 42%. It is possible that these two genes evolved independently to accept BRs. Although AtST1 and AtST4a accept BRs, it is possible that they perform different functions in *Arabidopsis* due to the differences in their substrate specificities and induction patterns. Recently, two other *Arabidopsis* STs have been identified in the TAIR database, AtST4b and AtST4c, which share between 75% and 83% amino acid identity with AtST4a. Due to the high identities shared by these three enzymes, both AtST4b and AtST4c, may have similar substrate specificities to AtST4a and should be tested with BRs to confirm this.

Biochemically, AtST1 and AtST4a behave differently with respect to substrate specificity. AtST1 preferentially accepts early BR precursors but does not accepts late-intermediate and end-products such as 24-epiCS and 24-epiBL. AtST1 also accepts a range of mammalian hormones and synthetic BRs to varying degrees (see section F, Annex). AtST4a, on the other hand, only accepts a variety of late-intermediate and end-product BRs, such as CS, BL, 24-epiCS, 24-epiBL, homoCS and homoBL.

AtST1 displays a relaxed stereospecificity as compared to BnST3, perhaps the result of an increased flexibility of the active site. While BnST3 will sulfonate estradiol with a 17β hydroxyl group, AtST1 will accept both 17β and 17α estradiol. However, AtST1 remains specific for the 22 hydroxyl position on epiBRs.

Unlike AtST1, AtST4a would not accept any of the mammalian hormones or early BR precursors. The enzymatic activity of AtST4a is not affected by the presence or

absence of the lactone moiety, nor is it affected by the oxidation state of position 6 on ring B. As no modifications are made to the side chain after the production of teasterone, it is likely that the activity of AtST4a is dependent upon the configuration of the A ring, which undergoes numerous modifications before conversion to BL.

The first modification to the A ring during BR biosynthesis occurs with the conversion of teasterone to typhasterol. At this point, the 3β-hydroxyl is epimerized to a 3α-hydroxyl. CS is then formed with the addition of a 2α-hydroxyl group. AtST4a first displays activity with CS and will not accept any other precursor, including teasterone. Therefore, it appears that the activity of AtST4a is dependent upon a dihydroxy α-configured A ring.

The opposite is observed with AtST1. AtST1 displays high relative activities with precursors with A rings in the β-configuration with activities sharply declining to undetecTable levels with BRs produced after teasterone. All of the mammalian hormones accepted by AtST1 either have a planar or β-configured 3-hydroxyl group. This suggests that AtST1 cannot sulfonate substrates with an α-configured A ring in the steroid backbone.

Such a dependence upon the A ring configuration is also observed with the human HSST when testing BRs (Table 7, Section F.2), and with the guinea pig HSSTs (Driscoll et al. 1993). The human HSST, like AtST1, accepts BR precursors with β-configured A rings and exhibits no activity with BRs possessing an α-configured A ring. Likewise, the α- and β- guinea pig HSST, only accept α- or β-configured 3-OH groups and do not accept planar 3-OH configurations.

Like BnST3, AtST1 is suspected of playing a role in BR degradation due to its specificity for a β-configured A ring and by its induction after pathogen attack. The role of AtST4a is less clear, but may also play a role in BR inactivation. AtST1 is specific for 24-epiBRs, whereas AtST4a accepts BRs and homoBRs. The presence of two genes encoding stereospecific BR STs in *Arabidopsis thaliana* suggests that BR stereoisomers, such as BL, homoBL and 24-epiBL, may play different roles in plant development, and that their activity requires independent regulation.

Alternatively, AtST4a may be involved in a transport mechanism similar to that for DHEA. DHEA is transported through the blood as a sulfate-conjugate bound to a steroid binding protein (SBP). It is acted on by sulfatases upon reaching target tissues where it regains its active properties. AtST4a only accepts BRs with an α-configured A ring which have biological activity. It is possible that AtST4a facilitates transport of these molecules from their site of biosynthesis to their site of action by increasing their water solubility via sulfonation.

E.1.3 Phenotypic Analyses of Transgenic Plants

It is clear from the analysis of the putative transgenic lines that there is a phenotype associated with the constitutive-expression of *AtST4a* in the sense orientation. The most severe dwarf phenotype is similar to the known dwarf phenotypes of BR-deficient mutant plants and suggests that the *in vivo* substrates of AtST4a are BRs. Furthermore, the range of phenotype observed is common to vacuum infiltrated lines and is due to differing T-DNA copy number and site of insertion. Generally, the phenotype is less pronounced with increasing gene copies due to a phenomenon known as co-

suppression. The observed phenotype supports the hypothesis that AtST4a is involved in BR degradation. Transgenic plants constitutively expressing the anti-sense orientation of *AtST4a* could substantiate this hypothesis. If AtST4a is involved in a BR degradation mechanism, we do not expect to see a phenotype similar to *Det2* mutants. However, if AtST4a is involved in a BR translocation mechanism, we expect to see a phenotype similar to a BR-deficient mutant.

E.1.4 Prospective for Future Work

It is unclear whether AtST4a is involved in BR degradation or BR transport. To better understand this protein's function, it would be necessary to expand expression studies in order to analyze the conditions under which expression is taking place. *AtST4a* promoter fusions to a reporter gene could determine its *in vivo* expression and tissue distribution, possibly clarifying its gene product role in plant growth and development. Production of transgenic plants constitutively expressing *AtST4a* in the anti-sense orientation and identification of a phenotype associated with such a transgenic plant may help to elucidate the *in vivo* function of AtST4a. It will be necessary to know whether BR-sulfonates are accumulated in plants, therefore, new isolation and characterization methods must be developed.

E.2 *AtST6*

E.2.1 Molecular Characteristics

Although the screen for *AtST6* was unsuccessful in determining conditions under which the gene is expressed, it is known that the original cDNA was isolated from flower buds of *Arabidopsis thaliana* ecotype Columbia C24. Mature flower and silique samples did not contain *AtST6* mRNA transcript, therefore it appears that this gene may display both temporal and spatial regulation in developing flower tissues.

E.2.2 Enzymology of Alcohol Sulfonation

AtST6 displays a broad specificity for alcohol and plant-specific alcoholic compounds, accepting both primary and secondary alcohols. Due to this indiscriminate affinity toward alcohols, it was not possible to determine the natural *in vivo* substrate of AtST6 in this study, given the vast array of primary, secondary and tertiary alcohols naturally present in plants.

E.2.3 Prospective for Future Work

Due to the substrate specificity of AtST6 it is difficult to determine its *in vivo* substrate(s) through typical metabolic screening procedures. To better understand the function of this protein, it would be necessary to expand expression studies to analyze the conditions under which induction occurs. Production of transgenic plants constitutively expressing *AtST6* in the sense and anti-sense orientations may also provide useful insight

into the function of this gene product. Identification of a phenotype associated with such transgenic plants may help to clarify the *in vivo* function of AtST6.

F ANNEX

F.1 AtST1 Biochemistry

In order to define the role of AtST1, the activity of purified, recombinant AtST1 expressed in *E. coli* was studied (Parez Y – unpublished). AtST1 catalyzes the transfer of the [^{35}S]-labelled sulfonate group from the cosubstrate PAPS, to BRs and mammalian steroids. A summary of the biochemical data is presented in Tables 5 and 6. AtST1 displays enzymatic properties similar to BnST3 (Rouleau et al. 1999). AtST1 has a high affinity for 24-epicathasterone with an apparent K_m of 6.9 μM and a V_{max} of 57 pkatal mg^{-1}. AtST1 does not accept BRs such as 24-epiBL and BL, and has a low affinity for the synthetic BRs (22*S*, 23*S*)-28-HomoBL and (22*S*, 23*S*)-28-HomoCS at concentrations below 5 μM. AtST1 displayed an apparent K_m of 3 μM for PAPS, which is threefold higher than that of BnST3 (Rouleau et al. 1999).

Variations in enzymatic activity do exist between AtST1 and BnST3. AtST1 displays relative activities between 11 and 22% for mammalian estrogenic substrates, such as 17β-estradiol and β-estradiol-3-methylether at concentrations of 5 and 200 μM. On the other hand, BnST3 characteristically does not exhibit activity with either 17β-estradiol or β-estradiol-3-methylether at low concentrations but has strong relative activities at 200 μM concentrations (Rouleau et al. 1999). AtST1 also accepts estrone, 17α-estradiol and testosterone, all of which are not accepted by BnST3. As AtST1 accepts testosterone, 17α- and 17β-estradiol, it is likely that non-stereospecific sulfonation is taking place at position 17, whereas BnST3 is stereospecific for the 17-hydroxyl group in the β-position (Rouleau et al. 1999). AtST1 also sulfonates position 3 of dehydroepiandrosterone and pregnenolone.

Table 5

Kinetic parameters of recombinant AtST1 for the preferred substrates

Substrate	K_m (μM)	V_{max} (pkatal*mg^{-1})	V_{max}/K_m (pkatal*mg^{-1}*μM^{-1})
24-Epicathasterone	7	57	8.1
6-deoxo-24-Epicathasterone	2	4	2
17β-Estradiol	3.0	2	0.7
Dehydroepiandrosterone	1	1	1
Pregnenolone	13	5	0.4

Table 6

Substrate specificity of recombinant AtST1

Substrate [a]	Relative activity at 200 μM (%)	Relative activity at 5 μM (%)
24-Epicastasterone	9	12
24-Epicathasterone [b,c]	/	100
24-Epiteasterone	34	47
(22R, 23R)-28-Homocastasterone	10	12
(22R, 23R)-28-Homobrassinolide [d]	100	16
(22S, 23S)-28-Homocastasterone	84	32
22-deoxy-24-Epiteasterone	21	12
6-deoxo-24-Epicathasterone	49	41
(22S, 23S)-22,23-epoxy-24-Epiteasterone	10	12
22,23,24-Trisepicastasterone	75	11
17α-Estradiol	13	15
17β-Estradiol	11	16
β-Estradiol-3-methylether	22	13
Pregnenolone	48	34
Androstanediol	52	37
Dehydroepiandrosterone	51	16

[a] Substrates with relative activities of <10% are not included.
[b] Maximun specific activity equals 13 pkatal mg^{-1}.
[c] Substrate inhibition was observed and denoted by /.
[d] Maximun specific activity equals 20 pkatal mg^{-1}.

Data from Parez Y., 2000 (unpublished).

F.2 HSST Biochemistry

Table 7

Substrate specificity of recombinant human hydroxysteroid sulfotransferase (HSST)

Substrate [a]	Relative activity at 10 μM (%)
Dehydroepiandrosterone [b]	100
6-deoxo-24-Epicathasterone	54
22-deoxy-24-Epiteasterone	78
(22*S*, 23*S*)-22, 23-Epoxy-24-Epiteasterone	52
24-Epiteasterone	32

[a] The kinetic parameters determined for recombinant HSST were a K_m value of 5.0 μM and a V_{max} value of 40 pkatak*mg^{-1} for dehydrepiandrosterone, and a K_m value of 2.0 μM for PAPS.
[b] Maximun specific activity equals 30 pkatal*mg^{-1}.

Data from Schinas A-M., 1998 (unpublished).

G REFERENCES

Aksoy IA, Otterness DM, Weinshilboum RM (1993a) Cholesterol sulfation in human liver: catalysis by dehydroepiandrosterone sulfotransferase. *Drug Metab. Dispos.* 21: 268-276.

Aksoy IA, Wood TC, Weinshilboum RM (1993b) Human liver estrogen sulfotransferase (EST): polymerase chain reaction (PCR) cloning of cDNA. *Biochem. Biophys. Res. Commun.* 4: 181.

Azpiroz R, Wu Y, LoCascio JC, Feldmann KA (1998) An *Arabidopsis* brassinosteroid-dependent mutant is blocked in cell elongation. *Plant Cell* 10: 219-230.

Baker B, Zambryski P, Staskawicz B, Dinesh-Kumar SP (1997) Signaling in plant-microbe interactions. *Science* 276: 726-733.

Barret-Conner E, Khaw KT, Yen SSCA (1986) Prospective study of dehydroepiandrosterone sulfate, morality, and cardiovascular disease. *New Eng. Jour. Med.* 315: 1519-1524.

Baumann E (1876) Ueber sulfosauren im harn. In *Ber. Dtsch. Chem. Ges.*, p. 54.

Benchtold N, Ellis J, Pelletier G (1993) In planta Agrobacterium mediated gene transfer by infiltration of adult *Arabidopsis thaliana* plants. *C.R. Acad. Sci. Paris, Life Sciences.* 316: 1194-1199.

Benveniste P (1986) Sterol biosynthesis. *Annu. Rev. Plant. Physiol.* 37: 275-308.

Birnboim HC and Doly J (1979) A rapid alkaline extraction procedure for screening recombinant plasmid DNA. *Nucleic Acids Res.* 7: 1513.

Bowman KG, Bertozzi CR (1999) Carbohydrate sulfotransferases: mediators of extracellular communication. *Chem. Biol.* 6: R9-R22.

Bradford MM (1976) A rapid and sensitive method for the quantitation of microgram quantities of protein utilizing the principal of protein-dye binding. *Anal. Biochem.* 72: 248-254.

Burnell JN, Anderson JW (1973) Adenosine 5'-sulfatophosphate kinase activity in spinach leaf tissue. *Biochem. Jour.* 134: 565-579.

Cashmore AR (1982) RNA extraction from plants. In *Methods in chloroplast molecular biology* (Edelman M, Hallick RB, Chua N.-H, eds.) Elsevier Biomedical Press, NY, pp 387-392.

Choe S, Dilkes BP, Fujioka S, Takatsuto S, Sakurai A and Feldmann KA (1998) The *DWF4* gene of *Arabidopsis* encodes a cytochrome P450 that mediates multiple 22α hydroxylation steps in brassinosteroid biosynthesis. *Plant Cell* 10: 231-244.

Choe S, Noguchi T, Fujioka S, Takatsuto S, Tissier CP, Gregory BD, Ross AS, Tanaka A, Yoshida S, Tax FE and Feldmann KA (1999) The Arabidopsis *dwf7/ste1* mutant is defective in the delta7 sterol C-5 desaturation step leading to brassinosteroid biosynthesis. *Plant Cell* 11: 207-221.

Choe S, Tanaka A, Noguchi T, Fujioka S, Takatsuto S, Ross AS, Tax FE, Yoshida S and Feldmann KA (2000) Lesions in the sterol delta reductase gene of Arabidopsis cause dwarfism due to a block in brassinosteroid biosynthesis. *Plant J.* 21: 431-443.

Choi Y-H, Fujioka S, Harada A, et al. (1996) A brassinolide biosynthetic pathway via 6-deoxocastasterone. *Phytochemistry* 43: 593-596.

Clarke CL, Adams JB, Wren BG (1982) Induction of estrogen sulfotransferase in the human endometrium by progesterone in organ culture. *Jour. Clin. Endocrin. Metab.* 55: 70-75.

Clouse SD, Langford M, McMorris TC (1996) A brassinosteroid-insensitive mutant in *Arabidopsis thalainan* exhibits multiple defects in growth and development. *Plant Physiol.* 111: 671-678.

Clouse SD, Hall AF, Langford M, McMorris TC and Baker ME (1993) Physiological and molecular effects of brassinosteroids on *Arabidopsis thaliana*. *J. Plant Growth Reg.* 12: 61-66.

Clouse SD (1997) Molecular genetic analysis of brassinosteroid action. *Physiol. Plant.* 100: 702-709.

Clouse SD, Feldmann K A (1999) Molecular genetics of brassinosteroid action. In *Brassinosteroids: Steroidal Plant Hormones* (Sakurai A, Yokota T and Clouse SD, eds.). Tokyo: Springer-Verlag, pp. 163-190.

Dalta RSS, Hammerlindl JK, Panchuk B, Pelcher LE, Keller W (1992) Modified binary plant transformation vectors with the wild-type gene encoding NPTII. *Gene* 211: 383-384.

Dalta RSS, Bekkaoui F, Hammerlindl JK, Pilate G, Dunstan DI, Crosby WL (1993) Improved high-level constitutive foreign gene expression in plants using an AMV RNA4 untranslated leader sequence. *Plant Sci.* 94: 139-149.

Doughty JK, Porter AJR, Morton AM (1991) Variation in the glucosinolate content of oilseed rape (*Brassica napus L.*) leaves. II. Response to infection by *Alternaria brassicae* (Berk.). *Ann. Appl. Biol.* 118: 469-477.

Driscoll WJ, Martin BM, Chen H-C, Strott CA (1993) Isolation of two distinct 3-hydroxysteroid sulfotransferases from the guinea pig adrenal. *Jour. Biol. Chem.* 268: 23496-23503.

Falany CN, Vazquez ME, Kalb JM (1989) Purification and characterization of human liver dehydroepiandrosterone sulfotransferase. *Arch. Biochem. Biophys.* 260: 641-646.

Falany CN, Vazquez ME, Heroux JA, Roth JA (1990) Purification and characterization of human liver phenol-sulfating phenol sulfotransferase. *Arch. Biochem. Biophys.* 278: 312-318.

Falany CN (1991) Molecular enzymology of human liver cytosolic sulfotransferases. *Trends Pharmacol. Sci.* 12: 255-259.

Falany CN, Krasnykh V, Falany JL (1995) Bacterial expression and characterization of a cDNA for human liver estrogen sulfotransferase. *Jour. Steroid Biochem. Mol. Biol.* 52: 529-539.

Falany CN (1997) Enzymology of human cytosolic sulfotransferases. *FASEB Jour.* 11: 206-216.

Faulkner IJ, Rubery PH (1992) Flavonoids and flavonoid sulfates as probes of auxin transport regulation in *Cucurbila pepo* hypocotyl segments and vesicles. *Planta* 186: 618-625.

Feldmann KA, Marks MD, Christianson ML, and Quatrano RS (1989) A dwarf mutant of *Arabidopsis* generated by T-DNA insertion mutagenesis. *Science* 243: 1351-1354.

Fujioka S, Choi Y-H, Takatsuto S, Yokota T, Li J, Chory J, Sakurai A (1996) Identification of castasterone, 6-deoxocastasterone, typhasterol and 6-deoxotyphasterol from the shoots of *Arabidopsis thaliana. Plant Cell Physiol.* 37: 1201-1203.

Fujioka S, Li J, Choi- Y-H, Seto H, Takatsuto S, Noguchi T, Watanabe T, Kuriyama H, Yokota T, Chory J and Sakurai A (1997) The Arabidopsis *de-etiolated2* mutant is blocked early in brassinosteroid biosynthesis. *Plant Cell* 9: 1951-1962.

Galbraith MN, Horn DHS, Middleton EJ, et al. (1969) The catabolism of crustecdysone in the blowfly *Calliphora stygia. J. Chem. Soc. Commun.* 1969: 1134-1135.

Geri CE, Cacchini E, Giannakou ME, Covey SN, Miller JJ (1999) Altered patterns of gene expression in *Arabidopsis* elicited by cauliflower mosaic virus infection and by a CaMV gene VI transgene. *Mol. Plant Microb. Interact.* 12: 377-384.

Glendening TM, Poulton JE (1990) Partial purification and characterization of a 3'-phosphoadenosine 5'-phosphosulfate: desulfoglucosinolate sulfotransferase from cress (*Lepidium sativum*). *Plant Physiol.* 94: 811-818.

Grove MD, Spencer GF, Rohwedder WK, Mandava NB, Worley FJ, Warthen JD, Steffens GL, Flippen-Anderson JL and Cook JC (1979) Brassinolide, a plant growth-promoting steroid isolated from *Brassica napus* pollen. *Nature* 281: 216-217.

Hai T, Schneider B, Adam G (1995) Metabolic conversion of 24-*epi*-brassinolide into pentahydroxylated brassinosteroid glucosides in tomato cell. *Phytochemistry* 40: 443-448.

Hai T, Schneider B, Porzel A (1996) Metabolic conversion of 24-*epi*-castasterone in cell suspension cultures of *Lycopersicon esculentum*. *Phytochemistry* 41: 197-201.

Hanai H, Nakayama D, Yang H, Matsubayashi Y, Hirota Y, Sakagami Y (2000) Existence of a plant tyrosylprotein sulfotransferase: novel plant enzyme catalyzing tyrosine O-sulfation of preprophytosulfokine variants in vitro. *FEBS Lett.* 470: 97-101.

Hanson AD, Rathinasabapathi B, Chamberlin B, Gage DA (1991) Comparative physiological evidence that β-alanine betaine and choline-*O*-sulfate act as osmolytes in halophytic *Limonium* species. *Plant Physiol.* 97: 119-1205.

Hart RF, Renskeres KJ, Nelson EB, Roth JA (1979) Localization and characterization of phenol sulfotransferase in human platelets. *Life Sci.* 24: 125-130.

He Z, Wang Z.-Y, Li J, Zhu Q, Lamb C, Ronald P and Chory J (2000) Perception of brassinosteroids by the extracellular domain of the receptor kinase BRI1. *Science* 288: 2360-2363.

Heroux JA, Roth JA (1988) Pysical characterization of a monoamine-sulfating form of phenol sulfotransferase from human platelets. *Mol. Pharmacol.* 34: 29-33.

Hobkirk RH (1993) Steroid sulfation. *Trends Endocrinol. Metab.* 4: 69-74.

Huxtable JR (1986) *Biochemistry of Sulfur*. New York: Plenum Press, pp. 293-358.

Ish-Horowicz D and Burke JF (1981) Rapid and efficient cosmid cloning. *Nucleic Acids Res.* 9: 2989.

Jain JC, Grootwassink JW, Reed DW, Underhill EW (1990) Purification and properties of 3'-phosphoadenosine 5'-phosphosulfate: desulfoglucosinolate sulfotransferase from *Brassica juncae* cell cultures. *J. Plant Physiol.* 136: 356-361.

Kakuta Y, Pedersen LG, Carter CW, Negishi M, Pedersen LC (1997) Crystal structure of estrogen sulfotransferse. *Nat. Struc. Biol.* 4: 904-908.

Kauschmann A, Jessop A, Koncz C, Szekeres M, Willmitzer L and Altmann T (1996) Genetic evidence for an essential role of brassinosteroids in plant development. *Plant Jour.* 9: 701-713.

Kallas P, Meier-Augenstein W, Schildknecht H (1989) Turgorine-Neue phytohormone. *Naturwiss. Rundsch.* 42: 309-317.

Kallas P, Meier-Augenstein W, Schildknecht H (1990) The structure-activity relationship of the turgorin PLMF-1 in the sensitive plant *Mimosa pidica. Jour. Plant Physiol.* 136: 225-230.

Kehoe JW, Bertozzi CR (2000) Tyrosine sulfation: a modulator of extracellular protein-protein interactions. *Chem. Biol.* 7: R57-R61.

Kiehlbauch CC, Lam YF, Ringer DP (1995) Homodimeric and heterodimeric aryl sulfortransferases catalyze the sulfuric acid esterification of N-hydroyl-2-acetylaminofluorene. *Jour. Biol. Chem.* 270: 18941-18947.

Kim S-K (1991) Natural occurrences of brassinosteroids. In *Brassinosteroids – chemistry, bioactivity and applications* (Cutler HG, Yokota Y, Adam G, eds). ACS Symp. Ser. No. 474, Amer. Chem. Soc., Washington, DC, pp. 26-35.

Klahre U, Fujioka S, Yokota T, et al. (1997) Characterization of the *diminuto* mutant and genes regulated by brassinosteroids. *Proc. Plant Growth Reg. Soc. Amer.* 24: 99.

Kolbe A, Schneider B, Porzel A, et al. (1994) Pregnane-type metabolites of brassinosteroids in cell suspension cultures of *Ornithopus sativus. Phytochemistry* 36: 671-673.

Kolbe A, Schneider B, Porzel A, Voigt B, Krauss G and Adam G (1995) Acyl-conjugated metabolites of brassinosteroids in cell suspension cultures of *Ornithopus sativus. Phytochemistry* 38: 633-636.

Kolbe A, Schneider B, Porzel A and Adam G (1996) Metabolism of 24-*epi*castasterone and 24-*epi*brassinolide in cell suspension cultures of *Ornithopus sativus*. *Phytochemistry* 41: 163-167.

Kolbe A, Porzel A, Schneider B and Adam G (1997) Diglucosidic metabolites of 24-epi-teasterone in cell suspension cultures of *Lycopersicon esculentum* L. *Phytochemistry* 46: 1019-1022.

Kolbe A, Schneider B, Porzel A and Adam G (1998) Metabolic inversion of the 3-hydroxyl function of brassinosteroids. *Phytochemistry* 48: 467-470.

Koristas VM, Lewis JA, Fenwick GR (1991) Glucosinolate response of oilseed rape, mustard and kale to mechanical wounding and infection by cabbage stem flea beetle (*Psylliodes chrysocephela*). *Ann. Appl. Biol.* 118: 209-221.

Lachaise F, Lafont R (1984) Ecdysteroid metabolism in crab: *Carcinus maenas*. *Steroids* 43: 243-259.

Lacomme C, Roby D (1996) Molecular cloning of a sulfotransferase in *Arabidopsis thaliana* and regulation during development and in response to infection with pathogenic bacteria. *Plant Mol. Biol.* 30: 995-1008.

Li J, Nagpal P, Vitart V, McMoriss TC, Chory J (1996) A role for brassinosteroids in light-dependent development of *Arabidopsis*. *Science* 272: 398-401.

Li J, Biswas MG, Chao A, Russel DW and Chory J (1997a) Conservation of function between mammalian and plant steroid 5α-reductases. *Proc. Natl. Acad. Sci USA* 94: 3534-3539.

Li J, Chory J (1997b) A putative leucine-rich repeat receptor kinase involved in brassinosteroid signal transduction. *Cell* 90: 929-938.

Long S (1989) *Rhizobium*-legume nodulation: Life together in the underground. *Cell* 56: 203-214.

Lyon ES, Jakoby WB (1980) The identity of alcohol sulfotransferases with hydroxysteroid sulfotransferases. *Arch. Biochem. Biophys.* 202: 474-481.

Majewska MD (1995) Neuronal actions of dehydroepiandrosterone: possible roles in brain development, aging, memory, and effects. *Ann. N.Y. Acad. Sci.* 774: 111-120.

Mandava NB (1988) Plant growth-promoting brassinosteroids. *Annu. Rev. Plant Physiol. Plant Mol. Biol.* 39: 23-52.

Marsolais F, Varin L (1995) Identification of amino acid residues critical for catalysis and cosubstrate binding in the flavonol 3-sulfotransferase. *J. Biol. Chem.* 270: 30458-30463.

Mathur J, Molnar G, Fujioka S, Takatsuto S, Sakurai A, Yokota T, Adam G, Voigt B, Nagy F, Maas C, Schell J, Koncz C and Szekeres M (1998) Transcription of the *Arabidopsis CPD* gene, encoding a steroidgenic cytochrome P450, is negatively controlled by brassinosteroids. *Plant Jour.* 14: 593-602.

Matsubayashi Y, Sakagami Y (1999) Characterization of specific binding sites for a mitogenic sulfated peptide, phytosulfokine-alpha, in the plasma-membrane fraction derived from Oryza sativa L. *Eur. Jour. Biochem.* 262: 666-671.

Mitchell JW, Mandava N, Worley JF (1970) Brassins – a new family of plant hormones from rape pollen. *Nature* 225: 1065-1066.

Mulder G J, Jakoby WB (1990) Sulfation. In *Conjugation Reactions in Drug Metabolism* (Mulder GJ, ed.). London: Taylor and Francis, pp. 107-161.

Murashige T, Skoog F (1962) A revised medium for rapid growth and bioassays with tobacco tissue cultures. *Physiol. Plant* 15: 473-479.

Mushegian A, Koonin E (1995) A putative FAD-binding domain in a distinct group of oxidases including a protein involved in plant development. *Prot. Science* 4: 1243-1244.

Nebert DW, Nelson DR, Coon MJ, Estabrook RW, Feyereisen R, Fujii-Kuriyama Y, Gonzalez FJ, Guengerich FP, Gunsalus IC and Johnson EF (1991) The P450 superfamily: update on new sequences, gene mapping and recommended nomenclature. *DNA Cell Biol.* 10: 1-14.

Nishikawa N, Abe H, Natsume M, et al. (1995) Epimerization and conjugation of ^{14}C-labelled epibrassinolide in cucumber seedlings. *J. Plant Physiol.* 147: 294-300.

Noguchi T, Fujioka S, Choe S, Takatsuto S, Yoshida S, Yuan H, Feldmann KA and Tax FE (1999) Brassinosteroid-insensitive dwarf mutants of *Arabidopsis* accumulate brassinosteroids. *Plant Physiol.* 121: 743-752.

Nomura T, Kitasaka Y, Takatsuto S, Reid JB, Fukami M and Yokota T (1999) Brassinosteroid/sterol synthesis and plant growth as affected by *lka* and *lkb* mutations of pea. *Plant Physiol.* 119: 1517-1526.

Otterness DM, Wieben ED, Wood TC, Watson WG, Madden BJ, McCormick DJ, Weinshilboum RM (1992) Human liver dehydroepiandrosterone sulfotransferase: molecular cloning and expression of the cDNA. *Mol. Pharmacol.* 41: 865-872.

Poulton JE, Moller BL (1993) Glucosinolates. In *Methods in plant biochemistry* (Dey PM, Harborne JB, eds). Vol. 9, pp. 209-238, Academic Press, London.

Radominska A, Comer KA, Ziminak P, Falany J, Iscan M, Falany CN (1991) Human liver steroid sulfotransferase sulfates bile acids. *Biochem. Jour.* 273: 597-604.

Rivoal J, Hanson AD (1994) Choline-*O*-sulfate biosynthesis in plants. *Plant Physiol.* 106: 1187-1193.

Robbins MP, Lipmann F (1958) Separation of two enzymatic phases in active sulfate synthesis. *Jour. Biol. Chem.* 233: 681-695.

Rouleau M, Marsolais F, Richard M, Nicolle L, Voigt B, Adam G, Varin L (1999) Inactivation of brassinosteroid activity by a salicylate-inducible steroid sulfotransferase from *Brassica napus*. *Jour. Biol. Chem.* 274: 20925-20930.

Sakurai A, Yokota T, Clouse SD (Eds.) (1999) *Brassinosteroids: steroidal plant hormones*. Springer, Tokyo.

Sala C and Sala F (1985) Effect of brassinosteroid on cell division and enlargement in cultured carrot (*Daucus carota* L.) cells. *Plant Cell Rep.* 4: 144-147.

Sanger F, Niklen S, Coulson AR (1977) DNA sequencing with chain-terminating inhibitors. *Proc. Natl. Acad. Sci. USA* 74: 5463-5467.

Saraste M, Sibbald PR and Wittinghofer A (1990) The P-loop – a common motif in ATP- and GTP-binding proteins. *Trends Biochem. Sci.* 15: 430-434.

Satter RH (1990) Leaf movement: an overview of the field. In *The pulvinus: motor organ for leaf movement* (Satter RL, Gorton HL, Vogelman TC, eds). pp. 1-9, American Society of Plant Physiologists, Rockville, Md.

Schildknecht H, Schimacher K (1981) Ein hoch Wirksamer leaf movement factor aus *Acacia karroo*. *Chem.-Ztg.* 105: 287-290.

Schildknecht H, Meier-Augenstein W (1990) Role of turgorins in leaf movement. In *The pulvinus: motor organ for leaf movement* (Satter RL, Gorton HL, Vogelman TC, eds). pp. 101-129, American Society of Plant Physiologists, Rockville, Md.

Schneider B, Kolbe A, Porzel A and Adam G (1994) A metabolite of 24-*epi*-brassinolide in cell suspension cultures of *Lycopersicon esculentum*. *Phytochemistry* 36: 319-321.

Schumacher K, Chory J (2000) Brassinosteroid signal transduction: still casting the actors. *Curr. Opin. Plant Biol.* 3:79-84.

Schwartz AG, Witcomb JM, Nyce JW, Lewbart ML, Pashko LL (1988) Dehydroepiandrosterone and structural analogues; a new class of cancer chemopreventive agents. In *Advances in cancer research*. pp. 391-424, Academic Press, New York.

Shaw WH, Anderson JW (1972) Purification, properties and substrate specificity of ATP-sulfurylase from spinach leaf tissue. *Biochem. Jour.* 127: 237-247.

Song W-Y, Moore R, McLachlan JA, Negishi M (1995a) Molecular characterization of a testis-specific estrogen sulfotransferase and aberrant gene expression in obese diabetogenic C57BLKsJ-db/db mice. *Endocrinology* 136: 2477-2484.

Song W-Y, Wang G-L, Chen L-L, Kim HS, Pi LY, Holsten T, Gardner J, Wang B, Zhai WX, Zhu LH, Fauquet C and Roland P (1995b) A receptor kinase-like protein encoded by the rice disease resistance gene, *Xa21*. *Science* 270: 1804-1806.

Strott CA (1996) Steroid sulfotransferases. *Endocr. Rev.* 17: 670-697.

Suzuki H, Kim S.-K, Takahashi N, Yokota T (1993a) Metabolism of castasterone and brassinolide in Mung Bean explant. *Phytochemistry* 33(6): 1361-1367.

Suzuki H, Fujioka S, Takatsuto S, Yanagisawa T, Yokota T, Murofushi N and Sakurai A (1994a) Biosynthesis of brassinolide from teasterone via typhasterol and castasterone in cultured cells of *Catharanthus roseus*. *J. Plant Growth Regul.* 13: 21-26.

Suzuki H, Inoue T, Fujioka S, Takatsuto T, Yanagisawa T, Yokota T, Murofushi N and Sakurai A (1994b) Possible involvement of 3-dehydroteasterone in the conversion of teasterone to typhasterol in cultured cells of *Catharanthus roseus*. *Biosci. Biotech. Biochem.* 58: 1186-1188.

Suzuki H, Inoue T, Fujioka S, Saito T, Takatsuto S, Yokota T, Murofushi N, Yanagisawa T and Sakurai A (1995a) Conversion of 24-methylcholesterol to 6-oxo-24-methylcholesterol, aputative intermediate of the biosynthesis of brassinosteroids, in cultured cells of *Catharanthus roseus*. *Phytochemistry* 40: 1391-1397.

Suzuki H, Fujioka S, Takatsuto S, Yokota T, Murofushi N and Sakurai A (1995b) Biosynthesis of brassinosteroids in seedlings of *Catharanthus roseus*, *Nicotiana tabacum*, and *Oryza sativa*. *Biosci. Biotech. Biochem.* 59: 168-172.

Szekeres M, Nemeth K, Koncz-Kalman Z, Mathur J, Kauschmann A, Altmann T, Redei GP, Nagy F, Schell J and Koncz C (1996) Brassinosteroids rescue the deficiency of CYP90, a cytochrome P450, controlling cell elongation and de-etiolation in *Arabidopsis*. *Cell* 85: 171-182.

Takahashi T, Gasch A, Nishizawa N, Chua H-H (1995) The *DIMINUTO* gene of *Arabidopsis* is involved in regulating cell elongation. *Genes Dev.* 9: 97-107.

Varin L, Barron D, Ibrahim RK (1987) Enzymatic assay for flavonoid sulfotransferase. *Anal. Biochem.* 161: 176-180.

Varin L, Ibrahim RK (1989) Partial purification and characterization of three flavonol specific sulfotransferases from *Flaveria chloraefolia*. *Plant Physiol.* 90: 977-981.

Varin L, Ibrahim RK (1991) Partial purification and some properties of flavonol 7-sulfotransferases from *Flaveria bidentis*. *Plant Physiol.* 95: 1254-1258.

Varin L, Marsolais F, Brisson N (1995) Chimeric flavonol sulfotransferases define a domain responsible for substrate and position specificities. *J. Biol. Chem.* 270: 12498-12502.

Varin L, Marsolais F, Richard M, Rouleau M (1997a) Biochemistry and molecular biology of plant sulfotransferases. *FASEB J.* 11: 517-525.

Varin L, Chamberland H, Lafontaine JG, Richard M (1997b) The enzyme involved in the sulfation of the turgorin, gallic acid 4-*O*-(β-D-glucopyranosyl-6'-sulfate) is pulvini-localized in *Mimosa pudica*. *Plant Jour.* 12: 831-837.

Veronese ME, Burgess W, Zhu X, McManus ME (1994) Functional characterization of two human sulphotransferase cDNAs that encode monoamine- and phenol-sulphating forms of phenol sulphotransferase: substrate kinetics, thermal-stability and inhibitor-sensitivity studies. *Biochem. Jour.* 302: 497-502.

Weinshilboum RM, Otterness DM (1994) Sulfotransferase enzymes. In *Conjugation-deconjugation reactions in drug metabolism and toxicity* (Kauffman FC, ed.). Chapt. 22, "Handbook of experimental pharmacology" series, Vol. 112, pp. 45-78, Springer-Verlag, Berlin, Heidelberg.

Weinshilboum RM, Otterness DM, Aksoy IA, Wood TC, Her C, Raftogianis RB (1997) Sulfotransferase molecular biology: cDNAs and genes. *FASEB J.* 11: 3-14.

Whittemore RM, Pearce LB, Roth JA (1985) Purification and characterization of a dopamine-sulfating form of phenol sulfotransferase from human brain. *Biochemistry* 24: 2477-2482.

Winter J, Schneider B, Strack D and Adam G (1997) Role of a cytochrome P450-dependent monooxygenase in the hydroxylation of 24-*epi*-brassinolide. *Phytochemistry* 45: 233-237.

Yamada J, Morisaki M, Iwai K, Hamada H, Sato N and Fujimoto Y (1997) 24-Methyl and 24-ethyl-$\Delta^{24(25)}$-cholesterols as immediate biosynthetic precursors of 24-alkylsterols in higher plants. *Tetrahedron* 53: 877-884.

Yokota T, Ogino Y, Takahashi N (1990) Brassinolide is biosynthesized from castasterone in *Catharanthus roseus* crown gall cells. *Agric. Biol. Chem.* 54: 1107-1108.

Yokota T, Higuchi K, Kosaka Y, Takahashi N (1992) Transport and metabolism of brassinosteroids in rice. In: Karssen CM, van Loon LC, Vreugdenhil D (Eds.), Progress in Plant Growth Regulation, Kluwer Academic Publishers, Netherlands, pp. 298-305.

Yokota T, Nakayama M, Wakisaka T (1994) 3-Dehydroteasterone, a 3,6-diketobrassinosteroid as a possible biosynthetic intermediate of brassinolide from wheat grain. *Biosci. Biotech. Biochem.* 58: 1183-1185.

Yokota T (1997) The structure, biosynthesis and function of brassinosteroids. *Trends Plant Sci.* 2: 137-143.

Yokota T, Nomura T, Kitasaka Y (1997) Biosynthetic lesions in brassinosteroid-deficient pea mutants. *Proc. Plant Growth Reg. Soc. Amer.* 24: 99.